

Geology, volcanology and geochemistry

Garba IV and the *Melka Kunture Formation*.

A preliminary lithostratigraphic approach

Jean-Paul Raynal¹, Guy Kieffer², Guillaume Bardin³

with the collaboration of Geneviève Papy¹

The site of Garba IV is set by the Awash River, at the outlet of a small tributary of the Garba creek (Fig. 1). During the various excavation campaigns, several archaeological units were discovered: IV C, IV D, IV E, IV F and IV G. The oldest visible units stand at level of the minor river bed and are paralleled with those of the Gombore I site, which contain Oldowan occupations (Taieb 1974; Chavaillon and Piperno 1975).

No information is available for the lowest part of the stratigraphy which remains below the water level. It would be useful to have core samples of the deposits under the present Awash level to complete the stratigraphic column and obtain essential elements on the commencement of the sedimentation in the studied area.

On the left bank of the Awash River, the *Melka Kunture Formation* is overlain by the *Formation of Kella* which consists mainly of a series of non welded ignimbrites and associated tuffs (Fig. 2). Deposits at Garba IV belong to the lowest parts of the *Melka Kunture Formation* which consists mainly of the piling and imbedding of volcanic direct air-fall deposits and volcano-derived sediments in a general fluvial context (Fig. 3).

We used classical field and laboratory methods. Altitudes were measured with a theodolite and connected to the general levelling of Ethiopia. The description of sedimentary units uses Miall's terminology of architectures and facies (1978, 1992, 1996), keeping in mind that the scale of the outcrops limits considerably some interpretations. Granulometric compositions were established by mechanical sieving on the coarse (>2 mm) and fine fraction (<2 mm) of sediment and by laser micro-granulometry (Malvern 2600) at the Institute of Prehistory and Quaternary Geology of Bordeaux I University. Granulometric parameters and indexes are presented in Φ unities (Inman, 1952; Tab. 1 after Cas and Wright 1992). Microfacies have been described from large thin sections after impregnation of oriented samples with Guilloché method (1985).

1. *Université de Bordeaux I, Institut de Préhistoire et de Géologie du Quaternaire, UMR 5199 CNRS, Avenue des Facultés, F- 33405 Talence et GDR 1122 CNRS, France. jpraynal@wanadoo.fr.* 2. *UMR 6042 CNRS, Université Blaise Pascal, Maison de la Recherche, 4 rue Ledru, 63057 Clermont-Ferrand Cedex 1, Centre de Recherches Volcanologiques et GDR 1122 CNRS.* 3. *Résidence Parc des quatre seigneurs, 111 rue Francis Lopez, 34000 Montpellier, France. indyluck@hotmail.com*

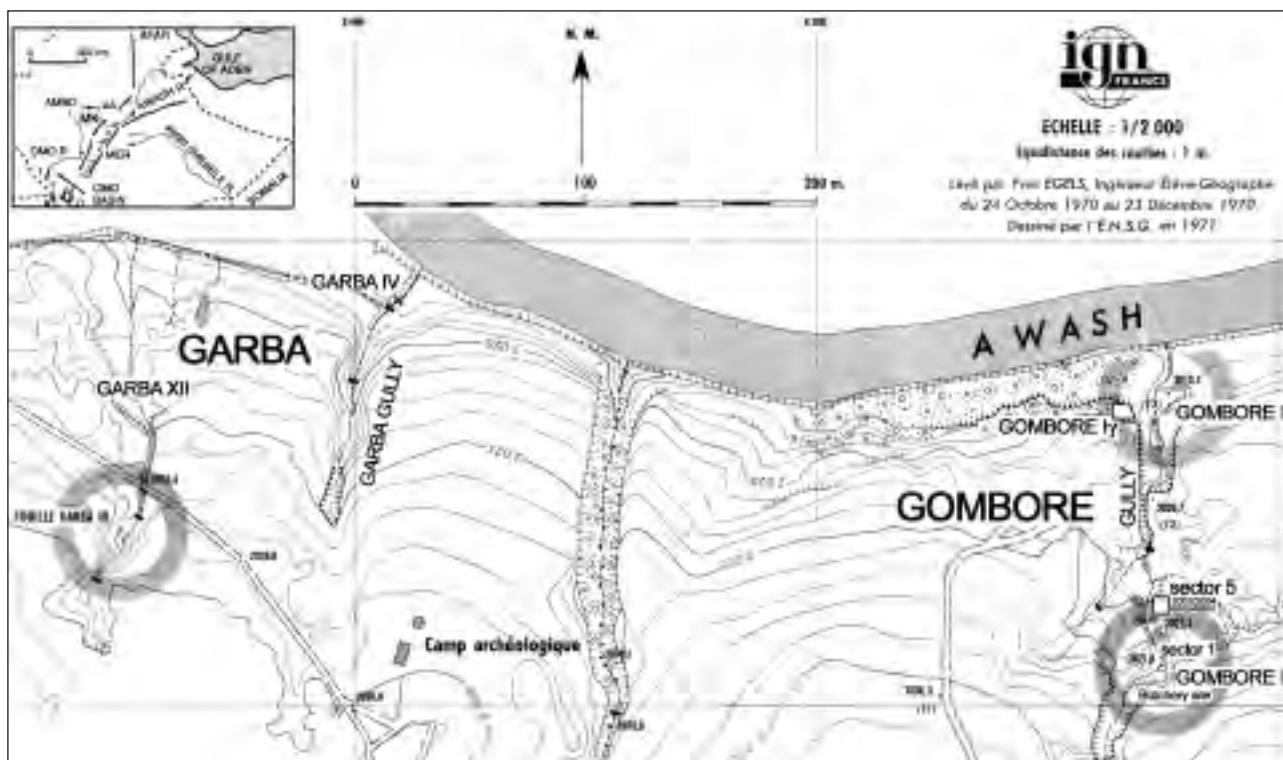


Fig. 1. Location map for the Melka Kunture area and detailed map of the Garba-Gombore sector (after Egels 1971).

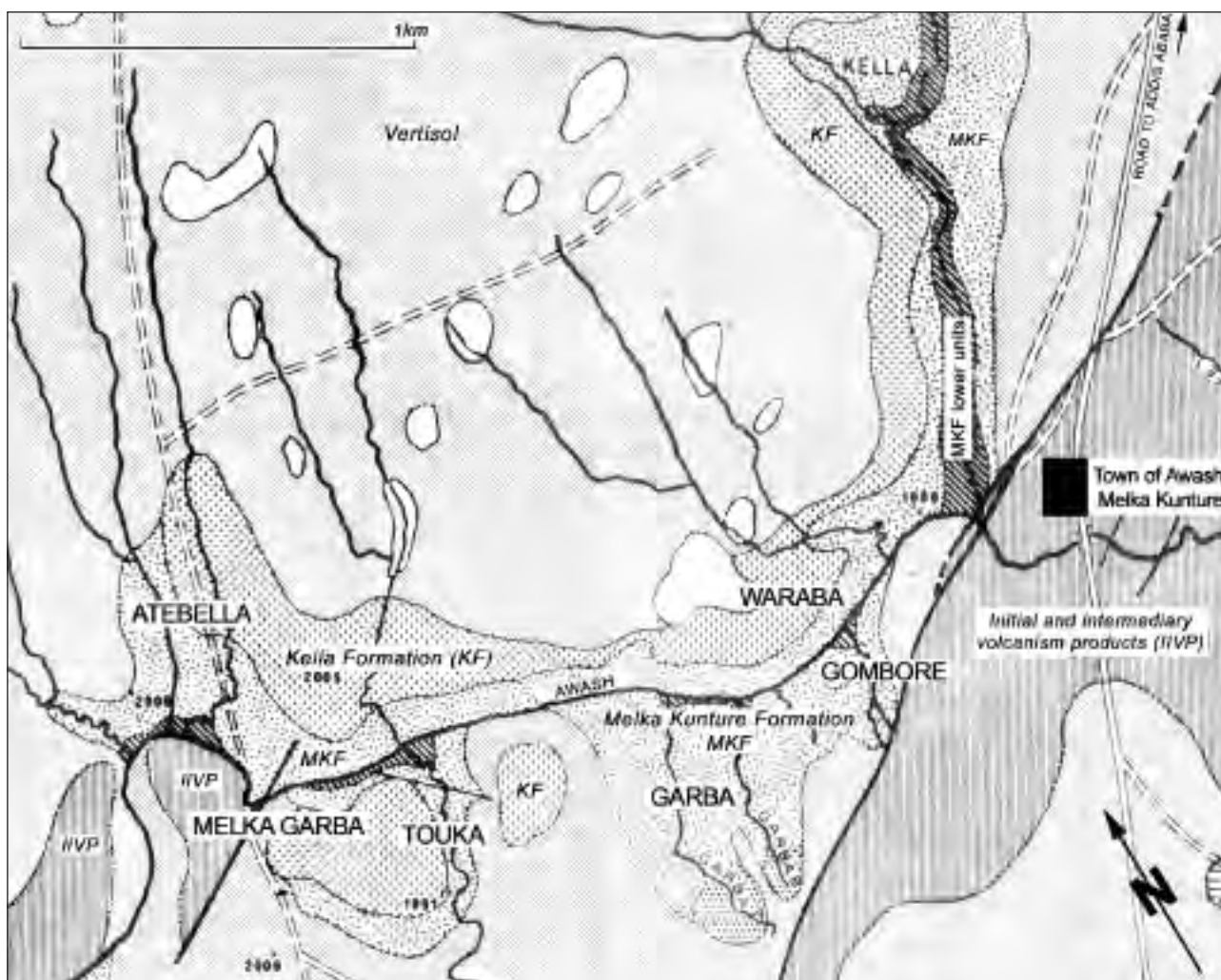


Fig. 2. Geological sketch map of the Melka Kunture area, after Täieb (1975) revised.

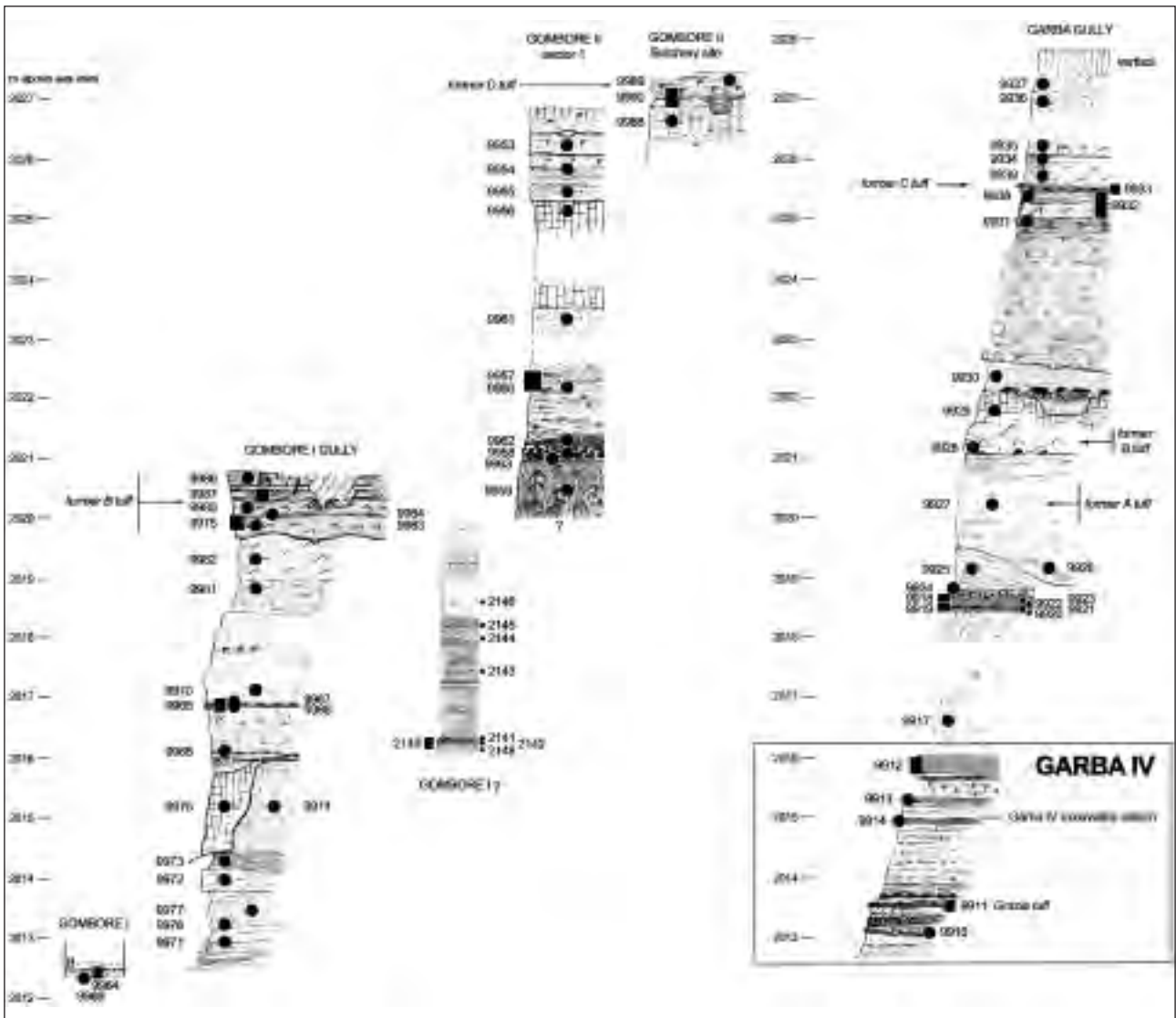


Fig. 3. Garba IV series in the context of the *Melka Kunture Formation* (logs in its lower part at Garba and Gombore).

Sorting σ_{ϕ}	Sedimentary deposits	Pyroclastic deposits
0 - 1	very well sorted to moderately sorted	very well sorted
1 - 2	poorly sorted	well sorted
2 - 4	very poorly sorted	poorly sorted
>4	extremely poorly sorted	very poorly sorted

Tab. 1 - Differences in descriptive summaries of sorting used by sedimentologists and volcanologists (after Cas and Wright 1992, p. 473).

Lithostratigraphy at Garba IV archaeological site

Sections have been examined at Garba IV where M. Piperno excavated a 6 m deep test pit near the other main excavation surface, close to the Awash River bank (Fig. 4). Both sections have been joined as they are only separated by a 25 to 30 cm thick layer of green sandy mud with soft pebbles and pumice observed during the site cleaning. From bottom to the top, one can observe a fluvial series 3.20 m thick with variations in major facies (Fig. 5). Even if the series is exclusively fluvatile and all the facies genetically linked, it seemed reasonable to divide it into three stratigraphic units.

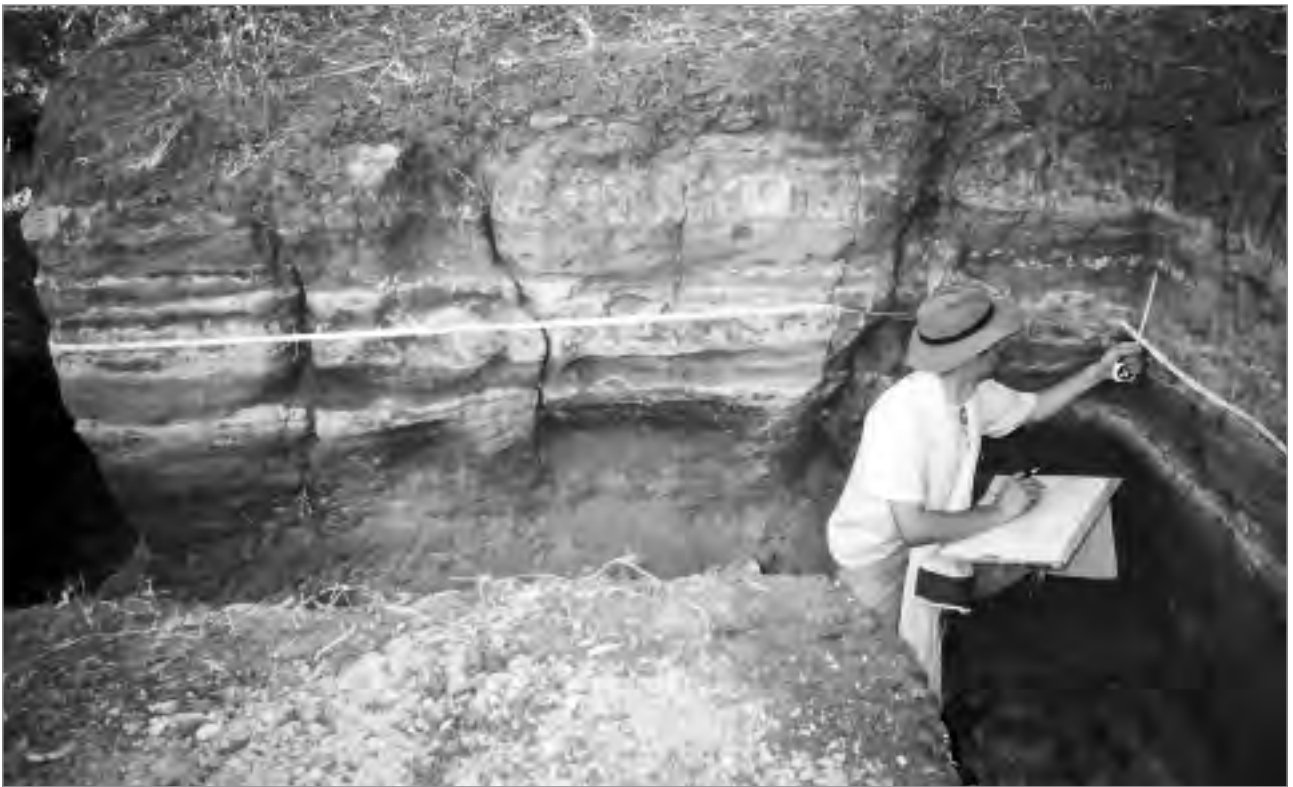


Fig. 4. Garba IV, section study on excavation walls above archaeological Layer D. *Cliché J.-P. Raynal*

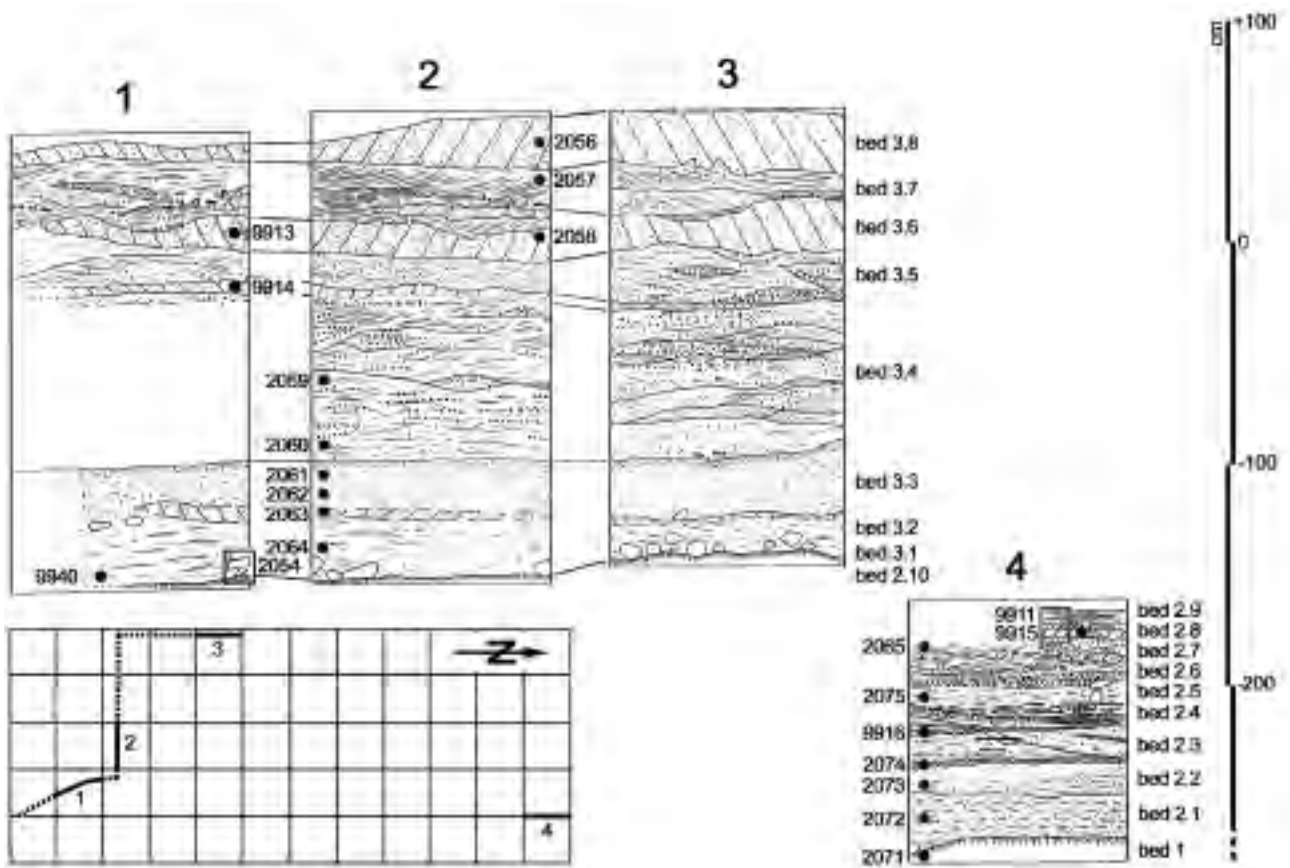


Fig. 5. Garba IV, stratigraphy and sampling locations.

Stratigraphic Unit 1

This stratigraphic unit is only represented by its summit (sample 2071). It is a bed of greenish silty-sands of imprecise thickness. The grain-size curve of this unit is plurimodal (Fig. 6) and the sorting is very poor ($Md_{\Phi} = 2.80$ and $\sigma_{\Phi} = 2.10$). The facies is of Sm type (Miall 1996), sediment-gravity flow deposit.

Stratigraphic Unit 2

Bed 2-1

This is deposit of silty sands (sample 2072), at most 25 cm thick. The grain-size curve of this unit is bimodal (Fig. 6) and the sorting is poor ($Md_{\Phi} = 2.95$ and $\sigma_{\Phi} = 1.37$). The facies is of Sm type (Miall 1996), sediment-gravity flow deposit. At the base of this deposit, some bone remains and ignimbrite pebbles occur. This may be the IV G archaeological Unit, discovered during former excavation campaigns and that lies at the base of the present Garba IV series.

Bed 2-2

Macroscopically, this is composed of light grey ashy sands (sample 2073), about 15 cm thick, more silty toward the base. The grain-size curve of this unit is bimodal (Fig. 6) and the sorting is very poor ($Md_{\Phi} = 2.75$ and $\sigma_{\Phi} = 2.10$). The facies is of Sm to Sh type (Miall 1996), sediment-gravity flow to plane-bed flow deposit.

Bed 2-3

This begins with a thin silty sand bed 2 to 3 cm thick (sample 2074) the base of which was affected with deformation as it was set down. The grain-size curve of this unit is bimodal (Fig. 5) and the sorting

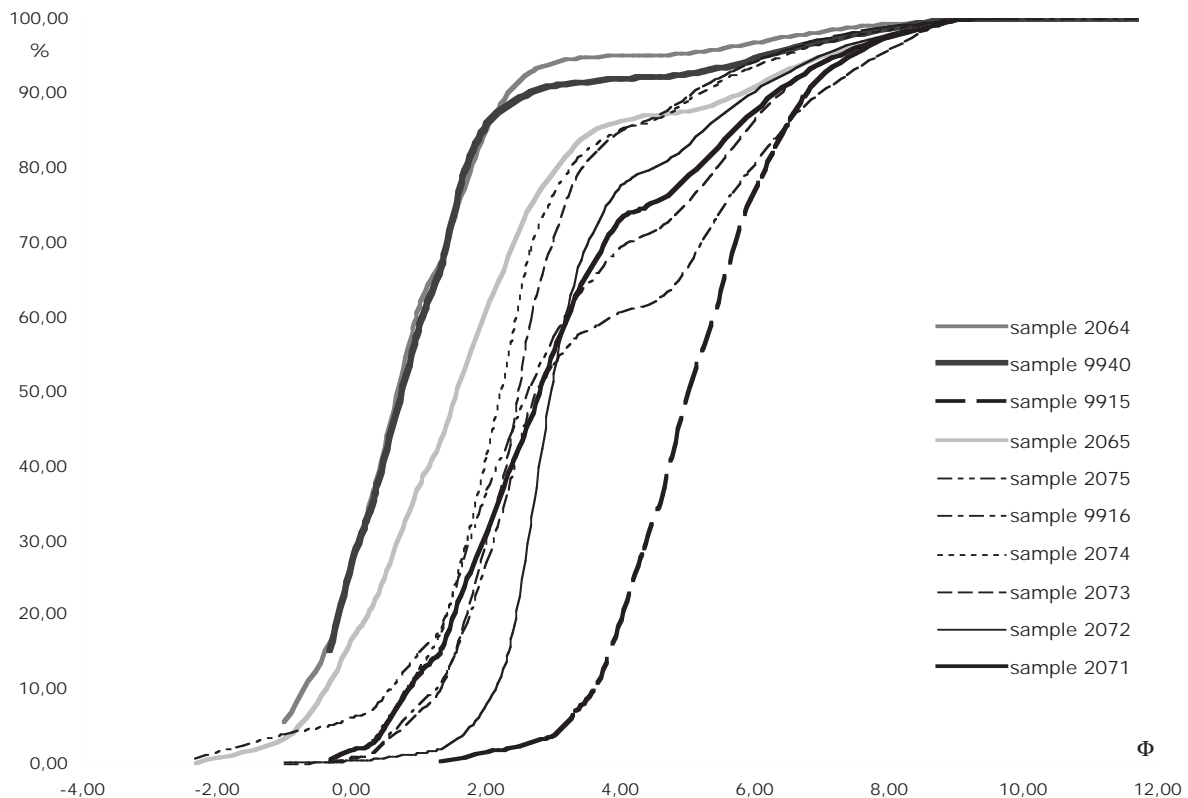


Fig. 6. Garba IV. Grain-size curves of lower beds up to archaeological Layer D.

is poor ($Md_{\Phi} = 2.20$ and $\sigma_{\Phi} = 1.25$). Then follow sands with sub-horizontal stratifications of Sh facies (Miall 1996) intercalated with grey lenses of silty sands (sample 9916) poorly sorted ($Md_{\Phi} = 2.75$ and $\sigma_{\Phi} = 2.37$) with a bimodal grain-size curve (Fig. 6). These deposits are obliquely crossed by oxidised black beds probably due to a phenomenon of sediment impregnation by a water table rich in metallic oxides or to a diffusion event.

Bed 2-4

A complex of more or less coarse reddish sands, commencing with a spindle shaped coarser unit. This unit, indurated with black metallic oxides, contains big pumices. The bedding is underlined by oxidised black bands.

Bed 2-5

This is a unit of fine grey pumiceous silty sands (sample 2075), laying directly on the indurated units beneath. The grain-size curve of this unit is bimodal (Fig. 6) and the sorting is very poor ($Md_{\Phi} = 2.60$ and $\sigma_{\Phi} = 2.32$). It contains the archaeological units IV F and IV E.

Bed 2-6

This is a gravel unit containing obsidian granules, indurated in its upper part by black metallic oxides.

Bed 2-7

This composed of pumiceous sands (sample 2065) coarsely stratified with beige silty cineritic beds showing deformations of a convoluted bedding type linked to the dynamics of the deposit. The bed is probably reworked ashy products coming from a distal fallout. The grain-size curve of this unit is bimodal (Fig. 6) and the sorting is poor ($Md_{\Phi} = 1.55$ and $\sigma_{\Phi} = 1.72$).

Bed 2-8 (tuff 9911)

This is a white tuff a few centimetres thick (see Raynal and Kieffer in this volume; sample 132 in Taieb 1974). The grain-size curve of this unit (sample 9915) is unimodal (Fig. 6) and the sorting is good ($Md_{\Phi} = 5.00$ and $\sigma_{\Phi} = 1.25$). This is a moderately distal direct fallout lightly reworked.

Bed 2-9

This is a unit of fine sand horizontally bedded with a coarser base fraction.

Bed 2-10

This is a green silty-sand unit of Sm facies on which lays the IV D archaeological unit.

Stratigraphic Unit 3

Bed 3-1

It is the IV D archaeological unit. It is constituted of bone fragments, blocks of welded ignimbrite and flaked artefacts. Because of its importance, we choose to consider it as a specific unit, contrary to other archaeological units. If this unit is a natural deposit, its facies should be Gcm (Miall 1996), clast supported massive gravel, or Gh.

Bed 3-2

These are bedded sands of facies Sh (Miall 1996), coarse to fine, including the IV D archaeological unit. The grain-size curves of this unit (samples 9940 and 2064) are unimodal (Fig. 6) and the sorting is moderate ($Md_{\Phi} = 0.70$ and $\sigma_{\Phi} = 1.10$).

A large thin section was cut in an oriented block of sediment extracted from bed 3-2 (sample 2054; Fig. 7). Under the microscope, one can observe at the bottom a large piece of welded ignimbrite with its classic vitreous fluidal porphyric structure (rust coloured oxidised glass, quartz and feldspath) contained in a conglomerate of various elements: bone fragments (Fig. 8), various minerals (quartz and feldspath; 1 mm) and fragments of various lava and ignimbrite (a few mm). One piece (>2 cm) of glass is partially in the course of vitrification with the beginning of a spherulitic structure. Elements are not connected and intergranular voids are visible. At the base, under the conglomerate with minerals and fragments of lava and ignimbrite, one can observe fine to pelitic material lightly disturbed belonging to bed 2-10. The upper part of the thin section shows the continuation (toward the top) of the composite micro-conglomerate of the lower part (average size of the elements: 1 to 2 mm): quartz and potassic feldspaths and plagioclases broken to subautomorphic, lava fragments and various ignimbrites, unconnected elements with no bedding (Fig. 9).

The upper part of bed 3-2 is made of finer cineritic sediment, which seems to carry the mark of an impregnation possibly by calcite.

Bed 3-3

A fine discontinuous tuffaceous silty bed forms the bottom part of this unit (sample 2063): the grain-size curve is plurimodal (Fig. 10) and the sorting is very poor ($Md_{\Phi} = 3.20$ and $\sigma_{\Phi} = 2.50$). The main body of this unit consists of coarse massive sands of Sm facies (Miall 1996). At their bottom (sample 2062), the grain-size curve is plurimodal (Fig. 10) and the sorting is moderate ($Md_{\Phi} = 0.20$ and $\sigma_{\Phi} = 1.05$). Then fine sands form the top part (sample 2061): the grain-size curve is still

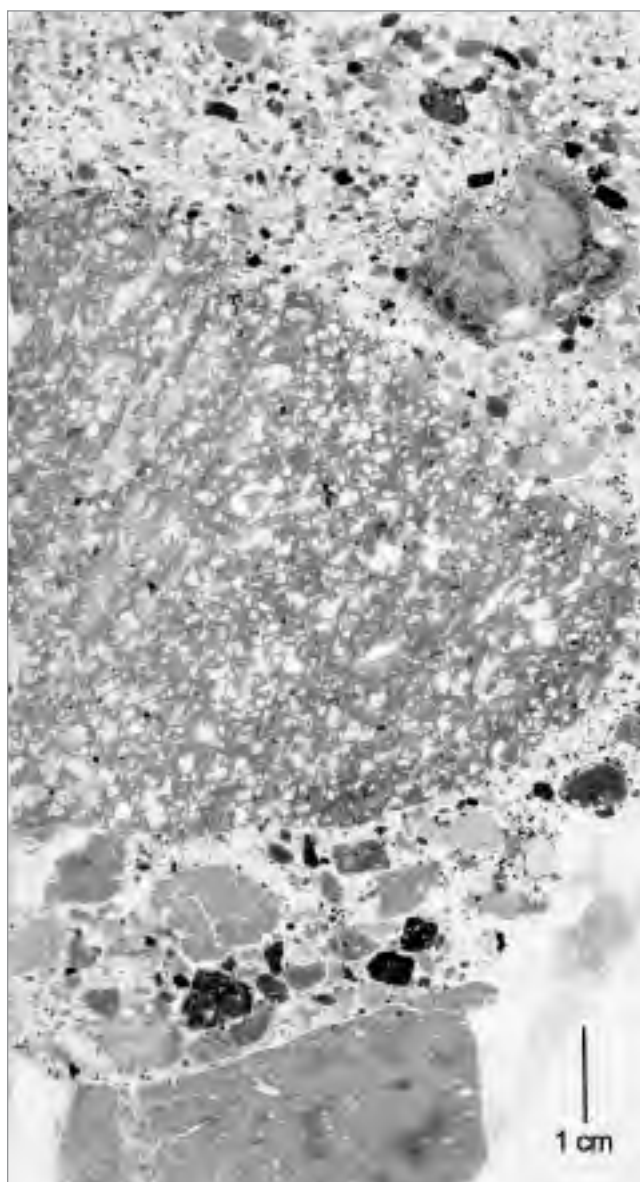


Fig. 7. Garba IV, sample 2054, thin section in beds 3.1 and 3.2, microscopic view in natural light.

Cliché J.-P. Raynal

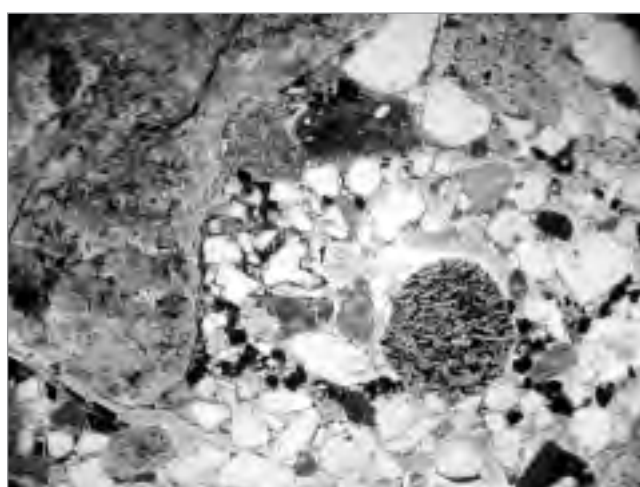


Fig. 8. Garba IV, sample 2054, thin section in bed 3.1, microscopic view in natural light, bone fragments in heterometric coarse sandy matrix. *Cliché J.-P. Raynal*

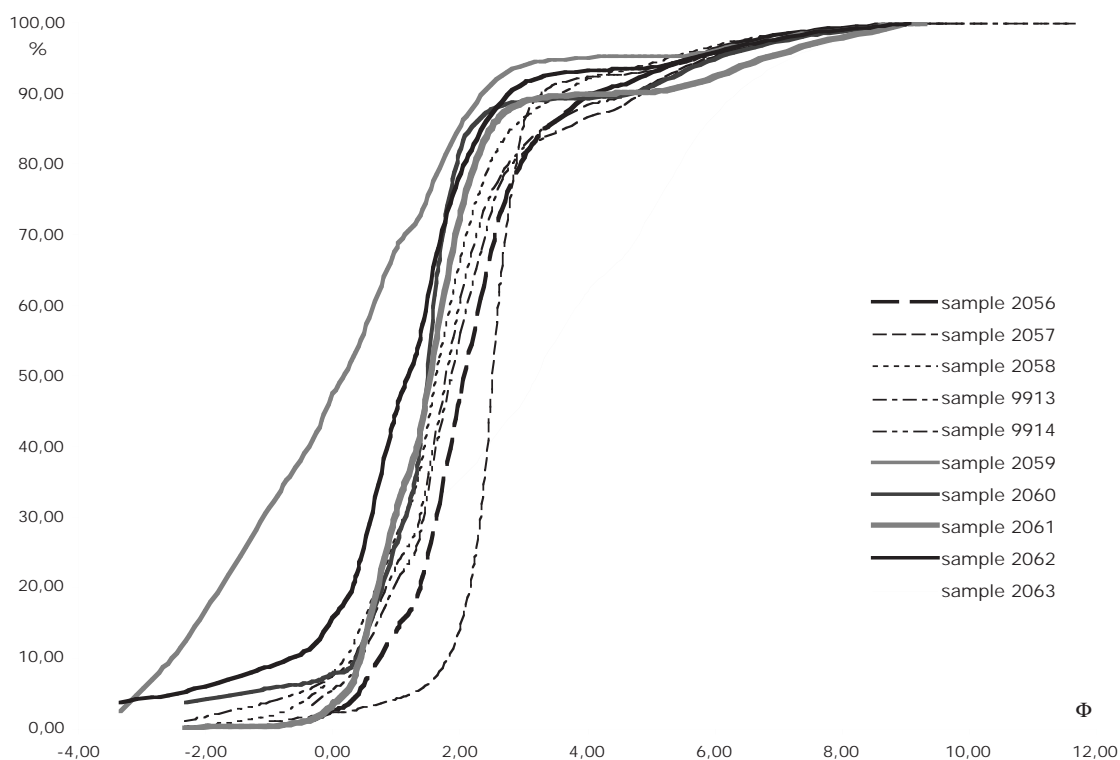


Fig. 10. Garba IV, grain-size curves of beds above archaeological Layer D.

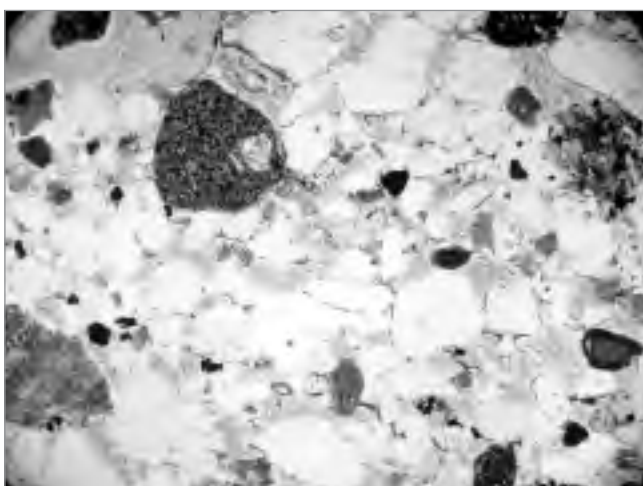


Fig. 9. Garba IV, sample 2054, thin section in bed 3.1, coarse sands, microscopic view in natural light.

Cliché J.-P. Raynal

plurimodal and the sorting is still moderate ($Md_{\Phi} = 1.50$ and $\sigma_{\Phi} = 0.90$; Fig. 10). Bed 3.3 contains the archaeological Unit IV C.

Bed 3-4

This unit shows 80 cm of coarse sands and gravels (sample 134 in Taieb 1974). At their bottom (sample 2060), the grain-size curve is bimodal (Fig. 10) and the sorting is moderate ($Md_{\Phi} = 1.50$ and $\sigma_{\Phi} = 0.75$). Some coarser lenses (sample 2059), show a plurimodal grain-size curve (Fig. 10) with a poor sorting ($Md_{\Phi} = 0.15$ and $\sigma_{\Phi} = 1.97$). The facies is St (Miall 1996) with fine interbedded stratifications, cradles and lenses (lateral evolution of temporary shallow channels, flow with light

transport capacity) eroding an underlying cinerite unit, producing soft pebbles. The transition from the preceding unit can be explained by a lateral move of the channel linked to an obstruction by volcanic mud.

Bed 3-5

This unit begins by a cinerite bed of irregular thickness. Then sands of St facies with cross-bedded stratifications, muddy tuffaceous beds and soft pebbles.

Bed 3-6

This is a unit of white redeposited cinerite variable in thickness and affected with deformation structures. It contains pockets of sandy material. The deposit mode is of muddy flow coulee type with surf fig-

ures. The grain-size curve of sample 2058 is bimodal (Fig. 10) and the sorting is moderate ($Md_{\Phi} = 1.60$ and $\sigma_{\Phi} = 1.10$).

Bed 3-7

At most 30 cm thick, this bed is a beige bank of sand with 20° oblique stratifications, of facies Sr (Miall 1996), which indicates a low flow regime. The grain-size curve (sample 2057) is bimodal (Fig. 10) but the sorting is good ($Md_{\Phi} = 2.50$ and $\sigma_{\Phi} = 0.37$). Inside this whole, are reworked soft pebbles, ripped from the underlying cinerite unit.

Bed 3-8

This is a white sandy cinerite, rather massive and spindle shaped, with a base affected by deformations of convoluted bedding type. The grain-size curve (sample 2056) is bimodal (Fig. 10) and the sorting is moderate ($Md_{\Phi} = 2.05$ and $\sigma_{\Phi} = 1.02$). Cinerites from beds 3.5 to 3.8 have been considered as a single reworked tuff unit 9914/12 (see Raynal and Kieffer in this volume).

Reconstitution of the sedimentary environments at Garba IV

The facies interpretation proposed here is mainly based on field observations (petrography and lithostratigraphy) and the study of thin sections made from samples taken during the 1999 survey.

The defined lithostratigraphic units show the following characteristics:

Unit 1 is only represented by its summit, that is of Sm facies (Miall 1996).

Unit 2 is characterised by rather fine sediments. It begins with silty-sands beds, becoming more and more sandy and in which we can find more silty beds and soft pebbles. The abundance of metallic oxide indurations and precipitations of carbonates impregnations indicates a sedimentary environment that could correspond to a low water basin in a minor bed, submitted to a contrasted hydric regime. It could also represent a temporary channel. In the upper part of this unit, a tuff bed occurs corresponding to a direct fallout, then back to a silty-sandy sedimentation, finishing with the bed of green silts marking the base of the archaeological Layer IV D.

These two stratigraphic units indicate an environment of flow sedimentation, affected by coarser sediments inflows during floods.

Unit 3 begins with fine tuffaceous sands, then continues with a series of coarse sands and gravels with cross-bedding stratifications. The cradle shapes correspond to in-filling of small channeled structures linked to a rather important dynamic. A finer sedimentation follows with sands containing oblique and planar stratifications, intersected with more or less thick sandy cineritic beds. The latter show a high degree of reworking. They probably occurred as episodic muddy flows.

These stratigraphic units show a vertical variation of their facies conveying an evolution of the river's hydrodynamic characteristics. Each time, these commence with silty-sandy sedimentation, then pass to a coarser sedimentation, before returning to a sedimentation of calmer environment.

This could correspond to what occurs in a system of channels with low sinuosity and a sandy dominance (Galloway and Hobday 1983). The channels with low sinuosity form in fluvial systems rich in either sandy or silty material. Each is characterised by a certain type of filling facies. The channels with low sinuosity rich in sand, show a variety in their deposit structure that includes lateral bars (accretion zones), transverse and longitudinal ones. Lateral accretion zones (bars) or the alternation of sandy bars, border the banks of channels with low sinuosity. Such structures are exposed at low water levels and

washed over during floods when the coarser material can reach the surface of the sandy bar and be deposited there.

The primary structures show accretion stratifications of fore-set type with low dip and planar stratifications. The active sandy bars, which accrete downstream in mid-channel position are oriented transversally to the course of the stream. They are typical of braided streams with sandy beds.

During the high water period, sediment passes above the ridge, proceeds up the sandy bar and tumbles down its side, creating small “avalanches” or tabular oblique stratifications. So, we could well be seeing here a transverse sandy bar.

One of the difficulties was to know if the paleo-Awash was responsible for these deposits. At the level of Garba, during the time of the deposits observed in the stratigraphy, the Awash may have followed a structural EW line. Nowadays, it retains this general orientation. It remains difficult to say if we have deposits set up by one or another of the Awash arms or by a right-bank tributary. The latter is likely, for the dynamics of the deposit and the size of the sedimentary structures do not seem to reflect what should occur in an important river, assuming that the Awash had more or less the same regime as nowadays. It could also be one of its arms. We can then imagine that the Awash River at the time was very divided, with braided channels.

The presence of tuff and cinerite units within the stratigraphy and the omnipresence of eruptive sediments, witness an intense volcanic activity that continued during the setting up of the sediments, either as direct fallout like the tuff of the upper part Unit 2 or the important beds of sandy cinerites in Unit 3. Regularly covered with pumiceous and ashy distal volcanic fallouts during the humid season or during rains, the unconsolidated material deposited on the slopes was transported into the rivers and incorporated to the sediment. It was then deposited as sandy mud or cinerites that show ball-and-pillow and load structures, linked to the deposit dynamic. Finally the river reverts to its normal sedimentation regime, eroding the later deposits and tearing soft pebbles from the fine unconsolidated muddy beds.

The presence of channels, sandy bars and basins corresponds to a sedimentary environment with a facies of calm puddles set up during low water, and a facies of bars deposited during floods. The presence of archaeological units and the associated ignimbrite blocks, contrast with the granulometry of the surrounding sediment and that of the silty units on which they often lay (Unit IV D, Unit IV G).

Organisation of archaeological units at Garba IV and hypothesis on their setting

Concerning the archaeological units observed in the Garba IV section, we know that the bone and lithic remains are mixed with ignimbrite blocks that can reach 10 cm in diameter, the whole being buried under a sandy matrix. Most of the time, they stand at the top of a clayey bank (Unit IV D, Unit IV G).

It is unlikely that the ignimbrite pebbles were brought there by hominids, considering that they are not a usable raw material from which manufacture tools, flaking with unpredictable fracture patterns and easily disintegrating when struck. Several hypotheses concerning their deposition are possible (Fig. 11). Possibly it is a case of reworking, when a flood transported simultaneously archaeological material and ignimbrite blocks (by lateral deposition or transport in a high sediment capacity stream), which essentially excludes the anthropic intervention.

Perhaps after the water receded the hominids settled in the zone at the back of a sandy bar or ridge. They would have used the raw material available on the spot to manufacture lithic tools. In this case the bone remains probably belong to animals hunted or scavenged by hominids and consumed on the spot. This anthropic hypothesis for the genesis of the archaeological units seems the most probable in the Garba IV case.

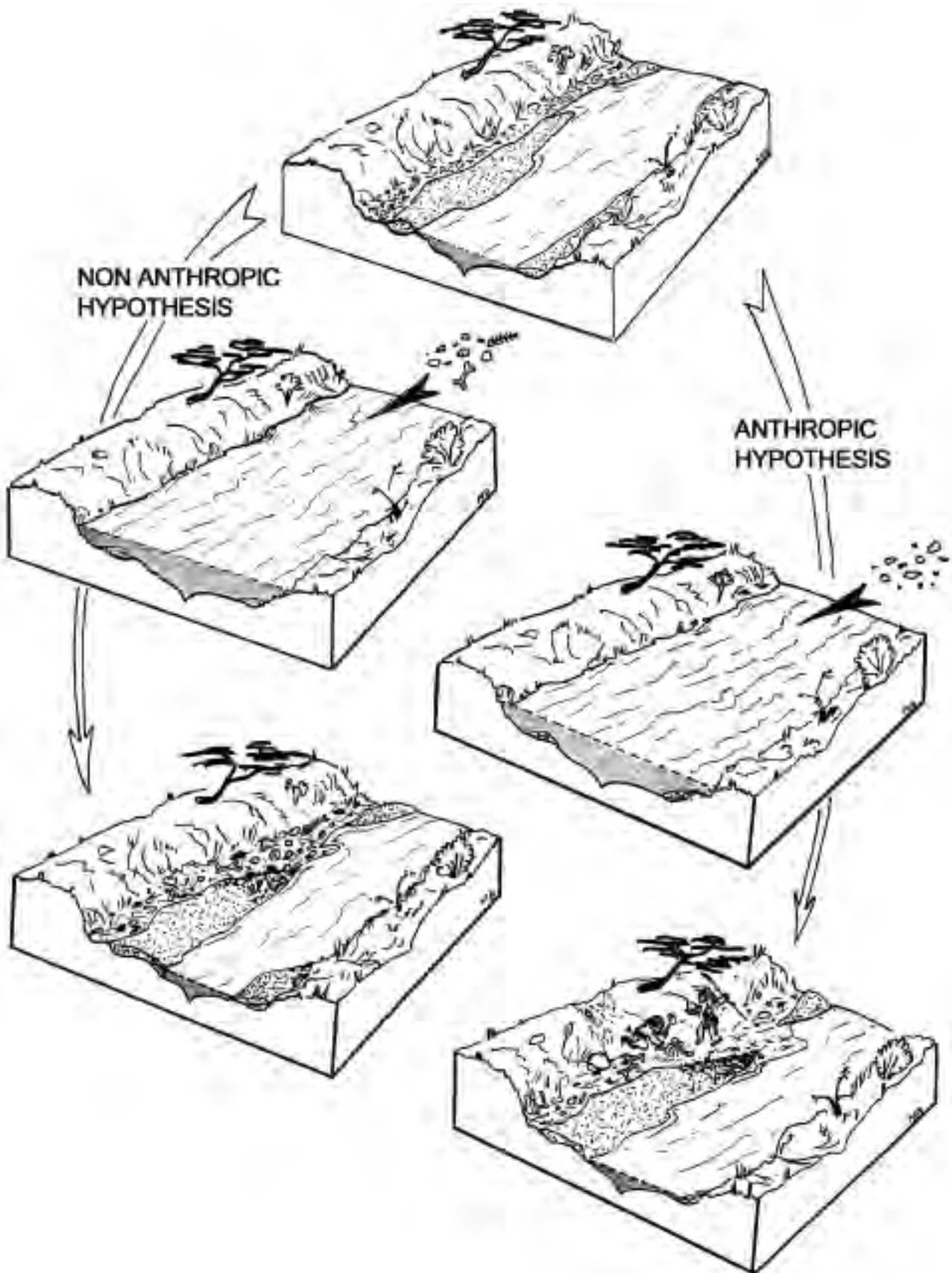


Fig. 11. Garba IV. Hypothesis about the formation of the site (after Bardin 2000).

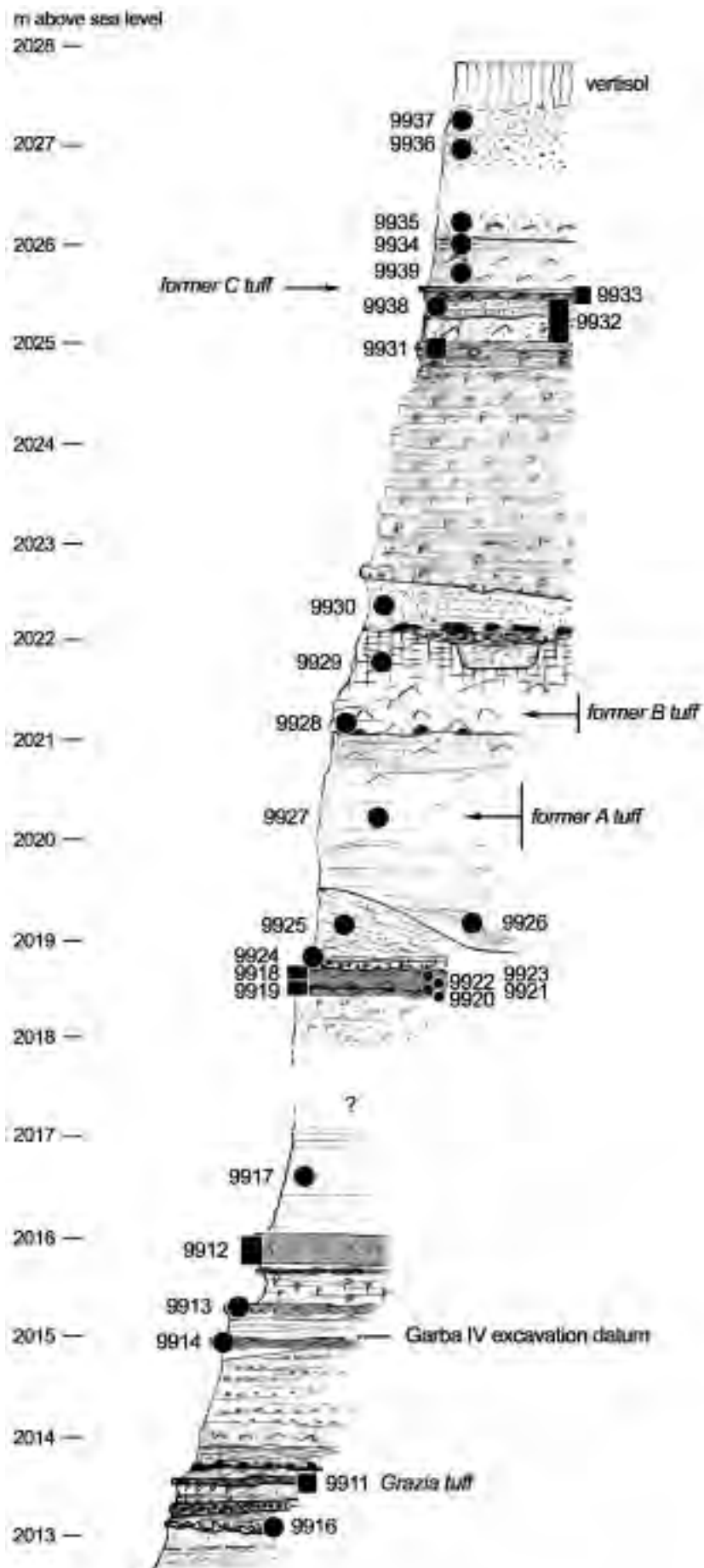


Fig. 12. The Garba IV and Garba Gully series: black dots are sediment samples in bulk; black rectangles are oriented blocks samples for examination under the microscope.

Naturally, this does not exclude a partial reworking of units after their initial deposition. A small part of the archaeological material (for instance bone fragments) could possibly have been reworked during another flood period.

The *Melka Kunture* Formation along Garba IV Gully

We examined sections along Garba IV Gully and reopened test pits at Garba XII (Fig. 1). The more recent sections which are located in the upper terms of the formation were not revised and are not considered in this paper. The extent and the limits of the complete formation have nevertheless been directly checked in a large area around Melka Kunture and our observations fit (with minor revisions) with the mapping established by Taieb (1974; Fig. 2). When this seems quite reasonable, we give the equivalence with the samples previously described (Taieb 1974). Above Bed 3.8 at Garba IV site and along Garba IV Gully we have observed the following succession (Fig. 12):

- Tephric sandy silts (sample 9917; sample 101 bis in Taieb 1974), observed on more than 1 m, plane bedded, Sh facies. The grain-size curve is plurimodal (Fig. 13) and the sorting is poor ($Md_{\Phi} = 5.15$ and $\sigma_{\Phi} = 1.87$).
- Cross-bedded coarse sands with obsidian gravels and pumice, 0.50 m at least, contact with lower unit not visible, St facies.
- Tuff unit 9919/18, 0.30 m, rhyolitic to dacitic magma (see Raynal and Kieffer in this volume), former A0 tuff of reverse polarity (Cressier 1980), K/Ar on glass shards at 1.30 and 1.46 Ma (Schmitt *et al.* 1977).
- Coarse sands and gravels with pumice, 0.10 m, Sl facies.
- Tuff unit 9924, 10 m, direct dacitic fall trapped in water (abundant shells of lamellibranchia; see Raynal and Kieffer in this volume).

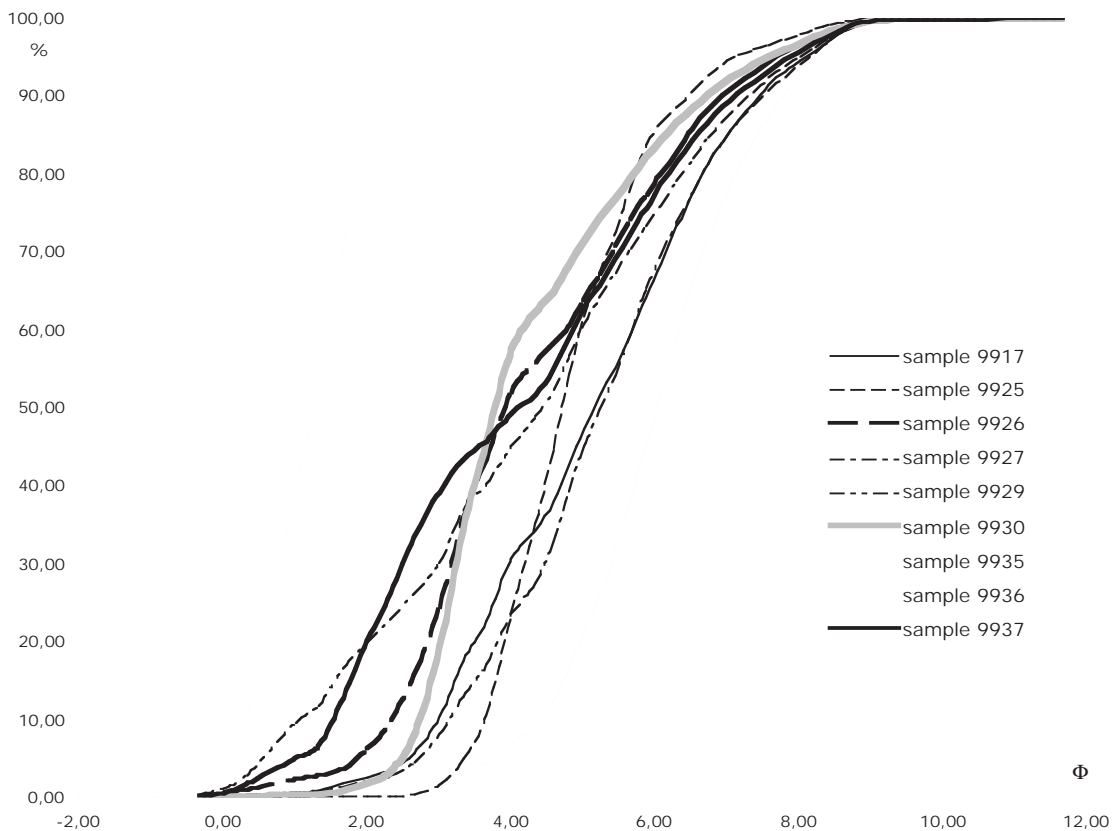


Fig. 13. Garba Gully, grain-size curves of the most representative layers.

- Trough cross beds of sandy silts, 0.70 m (sample 9925), St facies. The grain-size curve is unimodal (Fig. 13) and the sorting is moderate ($Md_{\Phi} = 4.70$ and $\sigma_{\Phi} = 1.02$). This unit is deeply eroded by the following deposit.
- Thick tephric sandy unit, 2.30 m at least, former A tuff of reverse polarity (Westphal *et al.* 1979; Cressier 1980), K/Ar on glass shards at 1.35 and 1.06 Ma (Schmitt *et al.* 1977) which thus indicate a maximum age for the emplacement of the sediment. This unit show clear figures of bioturbation. It begins with ripple cross-lamination (Sr facies) of silty-sands (sample 9926); the grain-size curve is bimodal (Fig. 13) and the sorting is poor ($Md_{\Phi} = 3.90$ and $\sigma_{\Phi} = 1.85$). They pass upwards to low angle cross-beds (Sl facies) of sands (sample 9927; sample 103 in Taieb 1974), the top of which is more silty; the grain-size curve is nearly unimodal (Fig. 13) and the sorting is still poor ($Md_{\Phi} = 5.25$ and $\sigma_{\Phi} = 1.67$). An erosional undulated surface truncates these deposits.
- Tuff unit 9928/29 with vegetal debris 1.00 m thick at least (sample 135 in Taieb 1974), previously named “tuff B” of reverse polarity (Westphal *et al.* 1979; Cressier 1980). Its base (sample 9928) consists of well sorted sandy silts ($Md_{\Phi} = 5.25$ and $\sigma_{\Phi} = 1.90$) corresponding to a fall (see Raynal and Kieffer in this volume); towards the top (sample 9929), silts are more sandy with a plurimodal grain-size curve (Fig. 13) and a very poor sorting ($Md_{\Phi} = 4.45$ and $\sigma_{\Phi} = 2.52$). At the very base, numerous pebbles belong probably to an archaeological layer. Granulometry, hydromorphy and vertic aspect of the top deposit of Sm to Fsm facies indicate a probable water-laid re-deposition and abandon of channel for the most part of this tuff unit.
- Preceding unit deposits is eroded by a narrow U-shaped channel (less than 1.00 m wide, 0.40 m deep) which is part of a larger channel (approximately 10.00 m wide). Coarse sands with gravels of St facies fill up the narrow channel which is capped by a line of Acheulian artefacts. Fine silty sands (sample 9930) of Sm facies have deposited above in the larger channel; their grain-size curve is plurimodal (Fig. 13) and their sorting is poor ($Md_{\Phi} = 3.75$ and $\sigma_{\Phi} = 1.55$).
- A larger channel of unknown extension (over 10.00 m wide) truncates the preceding unit and is filled up with low angle cross-beds (Sl facies) to planar cross-beds (Sp facies) of pumiceous sands (Unit 136 in Taieb 1974). Gravels can be seen at the base of the deposit, sometimes concentrated in small depressions.
- Tuff unit 9931/34, 1.00 m thick (Unit 129 in Taieb 1974), former tuff C of reverse polarity (Westphal *et al.* 1979; Cressier 1980) and rhyolitic composition (see Raynal and Kieffer in this volume).
- Silty and sandy unit, 1.30 m thick, Sm facies. At the bottom (sample 9935), poorly sorted tephric silts ($Md_{\Phi} = 6.00$ and $\sigma_{\Phi} = 1.27$) with a unimodal grain-size distribution (Fig. 13), certainly a reworked fall. At the top (sample 9936), well sorted sands ($Md_{\Phi} = 1.30$ and $\sigma_{\Phi} = 0.90$) with a faint planar bedding and a bimodal grain-size distribution, overlain by very poorly sorted silty sands (sample 9937; $Md_{\Phi} = 4.10$ and $\sigma_{\Phi} = 2.35$) with a faint planar bedding and a bimodal grain-size distribution (Fig. 13).
- Recent vertisol, 0.50 m.

The Melka Kunture Formation at Gombore

We examined sections at Gombore I and along Gombore Gully, at Gombore Iy, Gombore II (sector I and “Butchery site”), at Gombore II sector 5 (Fig. 1). When this seems quite reasonable, we give the equivalence with the units previously described (Taieb 1974). From the lowermost visible deposit, we have observed the following succession (Fig. 14).

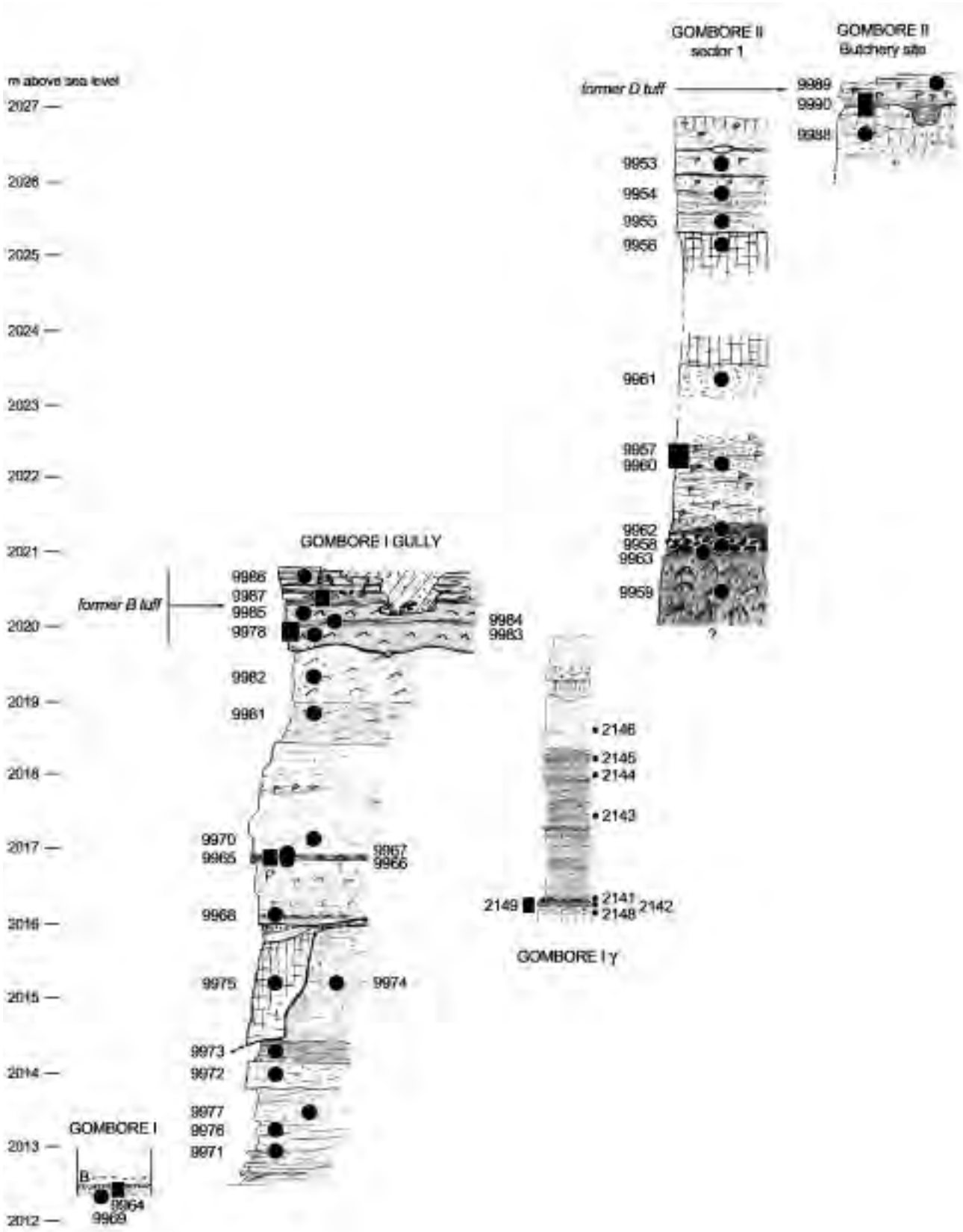


Fig. 14. The Gombore series: black dots are sediment samples in bulk, black rectangles are oriented blocks samples for examination under the microscope.

Gombore I site and Gombore I Gully

A test pit opened at Gombore I site show deposits below archaeological Layer B of Chavaillon excavations. They consist of:

- Silty coarse sands (sample 2147) very poorly sorted ($Md_{\Phi} = 1.10$ and $\sigma_{\Phi} = 2.42$) with a plurimodal grain-size curve and silty sands (sample 9969) poorly sorted ($Md_{\Phi} = 2.70$ and $\sigma_{\Phi} = 1.55$) with a plurimodal grain-size (Fig. 15). Facies is certainly Sh to Gh (Miall 1996) according to previous descriptions (Taieb 1974).
- A tuff unit (9945/47) existed between archaeological Layers B2 and B3 and was sampled by J. Chavaillon during his excavations at Gombore I. This silty-sandy tephric unit is a direct rhyolitic fall, quasi-identical to the "Grazia tuff" at the bottom of the Garba IV series (see Raynal and Kieffer in this volume). Polarity of the tuff itself has not been established but units below and above are considered as reverse (Cressier 1980).

We assume that preceding units form the bottom of the visible series even if there is nowadays no visible connection between these deposits and those preserved along the Gombore Gully sections which are from the bottom to the top:

- Sandy unit with silts and reworked tephra lenses, 1.30 m thick at least, low-angle cross-bedded, Sl to Sp facies (Miall 1996). Towards the base (sample 9971) very poorly sandy silts ($Md_{\Phi} = 4.80$ and $\sigma_{\Phi} = 2.35$) with a plurimodal grain-size curve; then well sorted sands (sample 9976; $Md_{\Phi} = 1.85$ and $\sigma_{\Phi} = 0.70$) with a unimodal grain-size curve; at the top, silty sands (sample 9977; $Md_{\Phi} = 2.60$ and $\sigma_{\Phi} = 2.27$) with a plurimodal grain-size curve (Fig. 15).
- Massive sandy-silty unit, 0.35 m thick, Sm facies (Miall 1996), poorly sorted sandy silts (sample 9972; $Md_{\Phi} = 4.75$ and $\sigma_{\Phi} = 1.92$) with a plurimodal grain-size curve (Fig. 15).

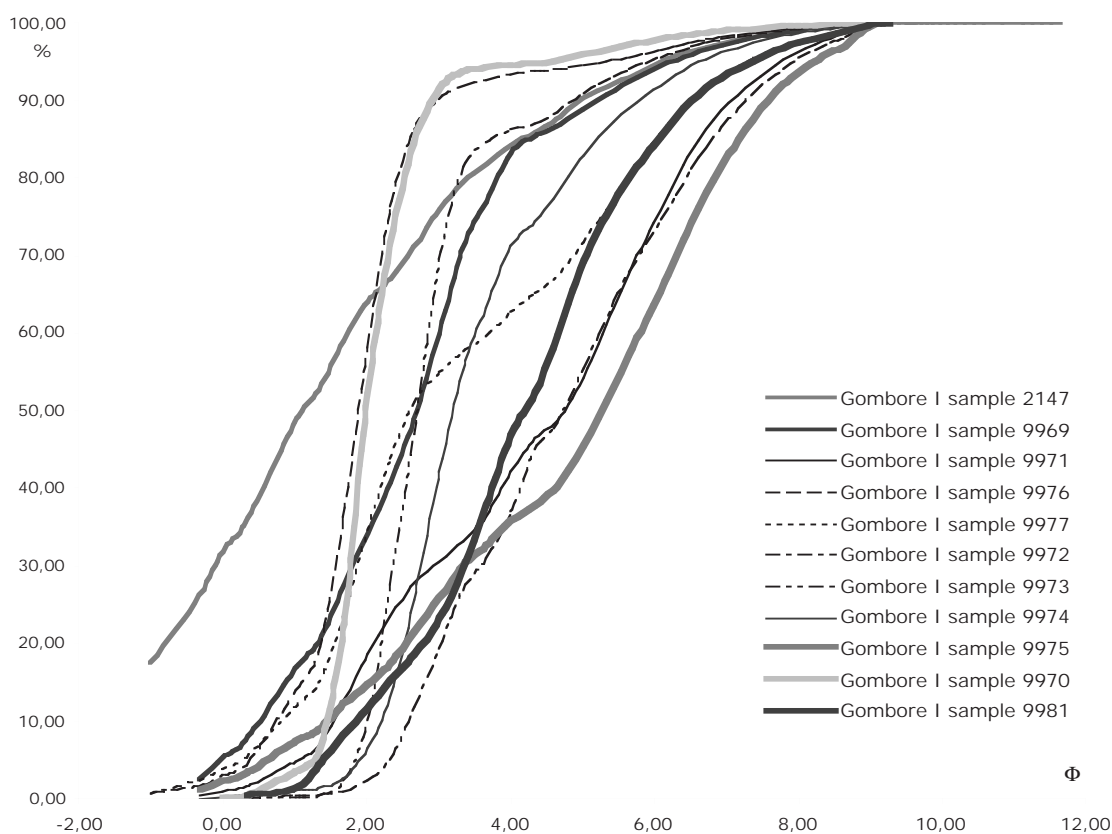


Fig. 15. Gombore I series, grain-size curves of the most representative layers.

- Cross-bedded sandy unit, 0.35 m thick, Sp facies (Miall 1996), well sorted silty sands (sample 9973; $Md_{\Phi} = 2.70$ and $\sigma_{\Phi} = 0.70$) with a bimodal grain-size curve (Fig. 15).
- Sandy unit, 1.60 m thick, Sm facies (Miall 1996), poorly sorted silty sands (sample 9974; $Md_{\Phi} = 3.20$ and $\sigma_{\Phi} = 1.35$; Fig. 15).
- Preceding units (an equivalent of sample 164 in Taieb 1974) are eroded by a U shaped channel, 2.00 m deep at least. Deposits in the channel and over-banking it are massive very poorly sandy silts 1.70 m thick of Fm facies (sample 9975; $Md_{\Phi} = 5.25$ and $\sigma_{\Phi} = 2.47$) with a plurimodal grain-size curve (Fig. 15). Top of the channel is slightly eroded by cross-bedded sands and gravels, 0.25 m thick, facies Gp (Miall 1996).
- Thick unit (2.50 m) of low-angle cross-bedded to planar bedded Sl to Sp facies (Miall 1996), very well sorted pumiceous sands (sample 9970; $Md_{\Phi} = 2.00$ and $\sigma_{\Phi} = 0.55$), with a unimodal grain-size curve (Fig. 15; sample 166 in Taieb 1974). These sands are interbedded with thin tuffs in primary position (9968 and 9965/67) and of dacitic to rhyolitic composition (see Raynal and Kieffer in this volume).
- Massive unit 1.35 m thick, Sm facies (Miall 1996), poorly sorted sandy silts (sample 9981; $Md_{\Phi} = 4.20$ and $\sigma_{\Phi} = 1.77$) with a bimodal grain-size curve in the lower part (Fig. 15); then poorly sorted less sandy silts (sample 9982; $Md_{\Phi} = 5.70$ and $\sigma_{\Phi} = 1.85$) with a bimodal grain-size curve in the upper part (Fig. 16; sample 167 in Taieb 1974). Both are considered as water-reworked falls (see Raynal and Kieffer in this volume).
- Tuff 9978/86, nearly 1.00 m thick (sample 167 in Taieb 1974). This unit settles on the preceding deposits by an undulated surge surface. The status of this tuff is still in debate. Despite several test pits and trenches, we never could clearly establish whether or not this unit, which overlies the Gombore I succession, precedes the Gombore II channel accumulation or is posterior to a late Lower Pleistocene

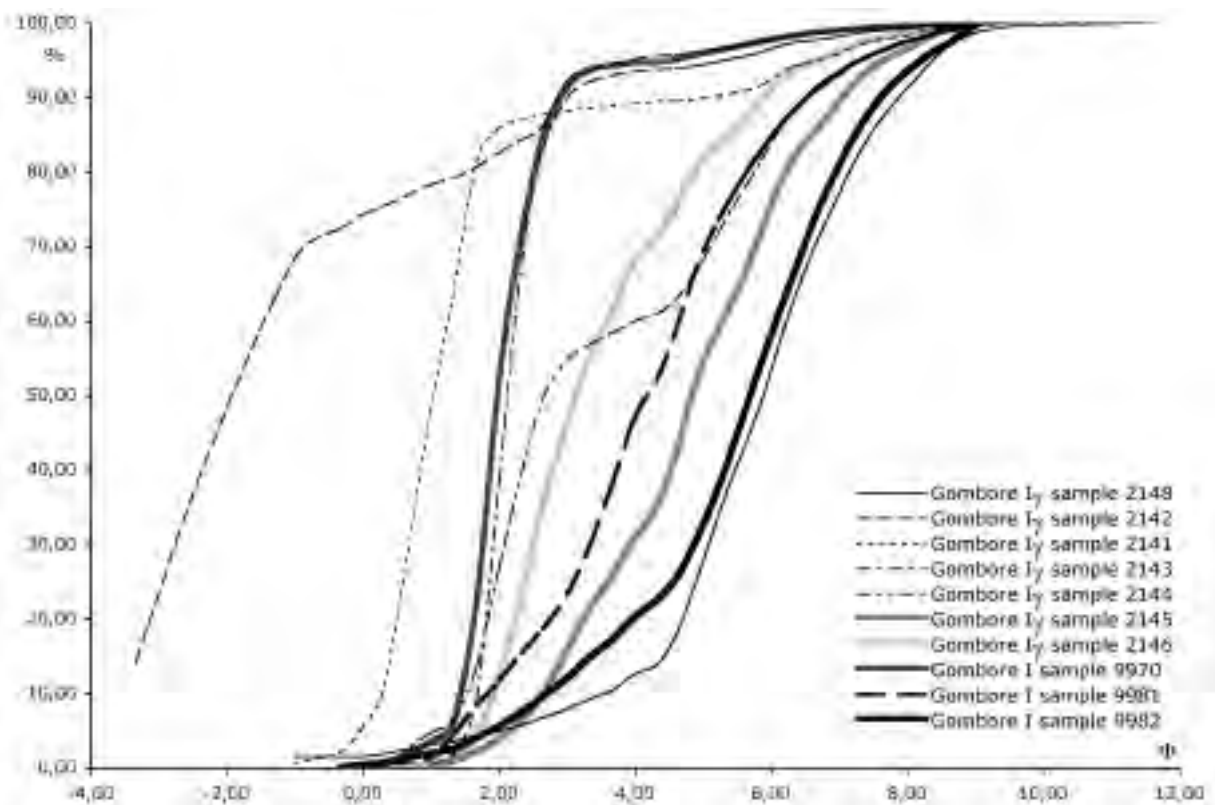


Fig. 16. Gombore I γ , grain-size curves of the most representative layers.

terracing of the Gombore area deposits. This rhyolitic to dacitic tuff has been identified previously as reverse “tuff B” (Chavaillon 1979c; Westphal *et al.* 1979; Cressier 1980), but no paleomagnetic data nor absolute dating was produced for the Gombore I outcrop.

Gombore I γ site

From the bottom to the top of the Gombore I γ section, we have observed the following succession (Fig. 14) which can be easily paralleled with the one observed in Gombore I Gully.

- Top of a massive unit of Fm facies (Miall 1996), 0.30 m thick, poorly sorted silts (sample 2148; $Md_{\Phi} = 5.90$ and $\sigma_{\Phi} = 1.45$) with a unimodal grain-size curve typical of decantation processes in an abandoned channel (Fig. 16). Under the microscope (sample 2149, bottom part; Figs. 17-19), we observe a detrital-pelitic environment (sludge or small broken crystals of quartz and feldspars, spots of black opaque oxides deposits, a few variations in grain size and dessication cracks. This unit is paralleled with deposits within the U-shaped channel described in Gombore I Gully succession.
- Clast supported massive sands and gravel unit, rich in obsidian, Gcm facies (Miall 1996), 0.10 m thick, very poorly sorted (sample 2142; $Md_{\Phi} = -1.90$ and $\sigma_{\Phi} = 2.77$), with a plurimodal grain-size curve (Fig. 16). Under the microscope (sample 2149, middle part), we observe a typical alluvial conglomerate with some round-shaped grains (about 1 cm), minerals (quartz, feldspars and clinopyroxenes) and mainly rolled fragments of lavas and various ignimbrites, obsidian and fibrous pumices (up to 3 cm in diameter). Tongues of this unit penetrate the dessication cracks of the lower detrital-pelitic unit (Figs. 18, 19). The archaeological layer belongs to this unit.
- Sandy unit 2.00 m thick, of low-angle cross-bedded to planar bedded S1 to Sp facies (Miall 1996). Under the microscope (sample



Fig. 17. Gombore I γ . Oriented sample 2149 prepared in archaeological layer and enclosing beds.

Cliché J.-P. Raynal

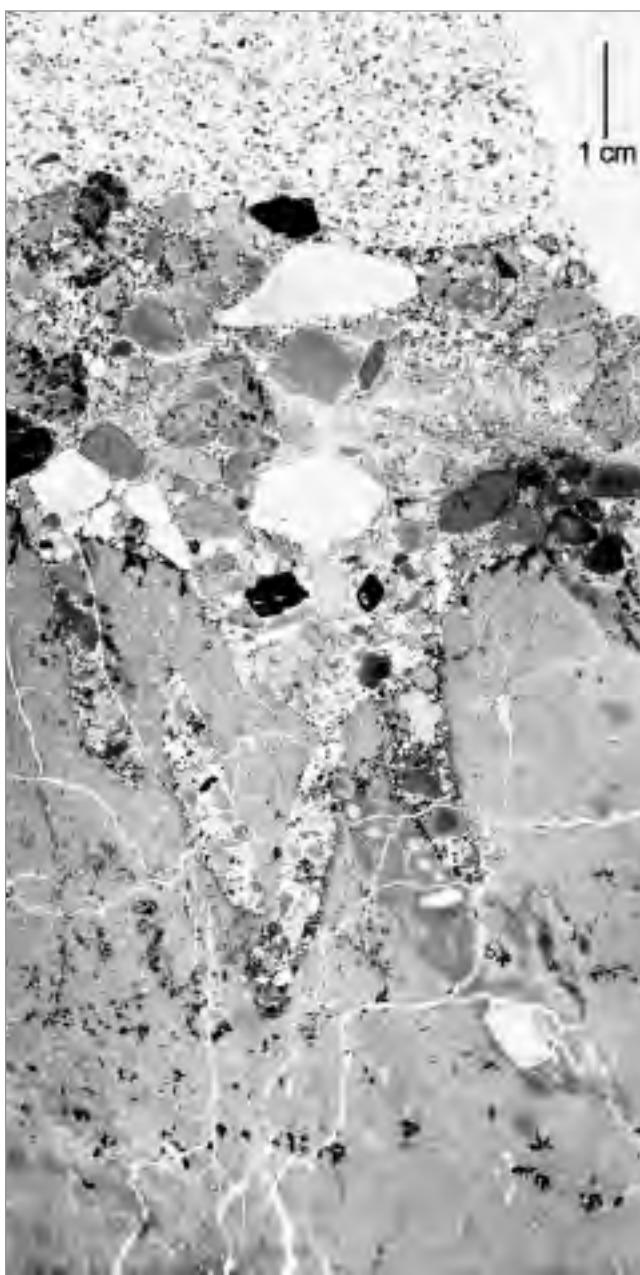


Fig. 18. Gombore I γ . Thin section from oriented sample 2149 in archaeological layer and enclosing beds, natural light. *Cliché J.-P. Raynal*

2149, top part) we observe at the base a neat superposition of epiclastic sands rich in minerals, fragments of various lavas and oxidised grains, quartz, potassic feldspars and plagioclases (Figs. 20, 21); these sands (sample 2141) are well sorted ($Md_{\Phi} = 1.05$ and $\sigma_{\Phi} = 0.67$) with a bimodal grain-size curve (Fig. 16). In the middle of the deposit, the sands of planar beds (sample 2143) are very well sorted ($Md_{\Phi} = 2.15$ and $\sigma_{\Phi} = 0.37$) with a unimodal extremely steep grain-size curve (Fig. 16). The top part of the unit (Fig. 22) shows very thin interbedded reworked tephric units, sandy and very poorly sorted (sample 2144; $Md_{\Phi} = 2.65$ and $\sigma_{\Phi} = 2.12$) with a bimodal grain-size curve, to silty and poorly sorted (sample 2145; $Md_{\Phi} = 4.85$ and $\sigma_{\Phi} = 1.75$) with a plurimodal grain-size curve (Fig. 16).

- Massive unit 0.70 m thick, Sm facies (Miall 1996), poorly sorted epiclastic sandy silts (sample 2146; $Md_{\Phi} = 3.15$ and $\sigma_{\Phi} = 1.57$) with a unimodal grain-size curve (Fig. 16).
- Unit 0.20 m thick of Fm facies (Miall 1996).
- Unit 0.60 m thick of clast-supported pumiceous and obsidian gravels, Gcm facies, passing upwards to sands of Sm facies (Miall 1996). This alluvium is very similar to the one at the bottom of Gombore II sector 5 section but the transition has not been directly established; if this was correct, the tuff complex 9978/86 at the top of Gombore I Gully would be encased in a more recent topography and belong to a late Lower Pleistocene volcanic episode. We need more investigations in this area between Gombore I γ and Gombore II.

Gombore II sector 5

The reopening of a large excavation at Gombore II sector 5 (Fig. 1) has allowed detailed observations of the microsedimentary context below and above an Acheulian archaeological surface.

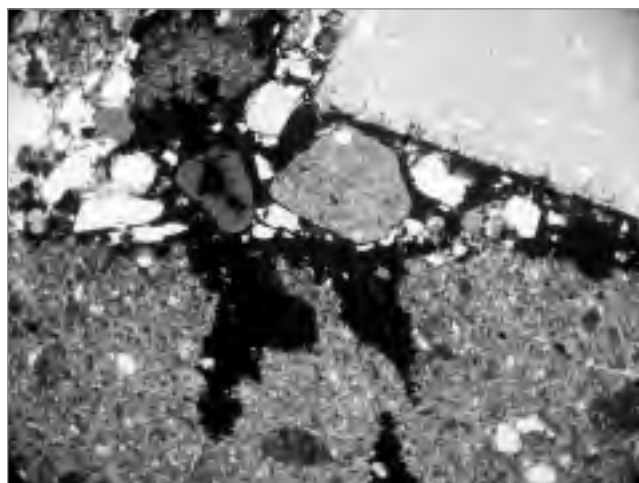


Fig. 19. Gombore I γ , microscopic view of sample 2149, silty sands with dessication cracks overlain by the archaeological layer, natural light. *Cliché J.-P. Raynal*

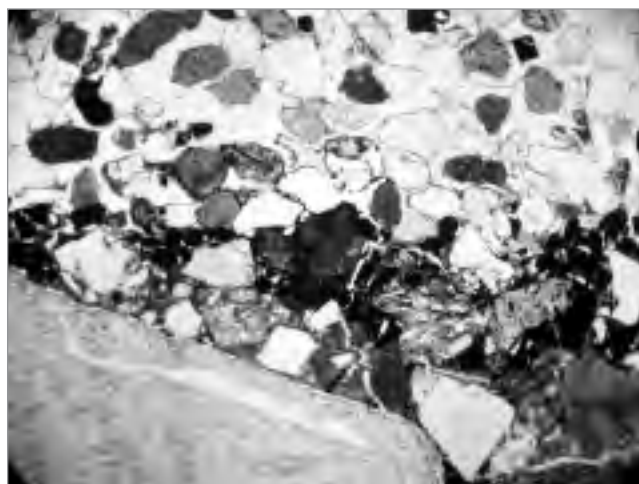


Fig. 20. Gombore I γ , microscopic view of sample 2149, the transition between the archaeological layer and the overlying sands, natural light. *Cliché J.-P. Raynal*

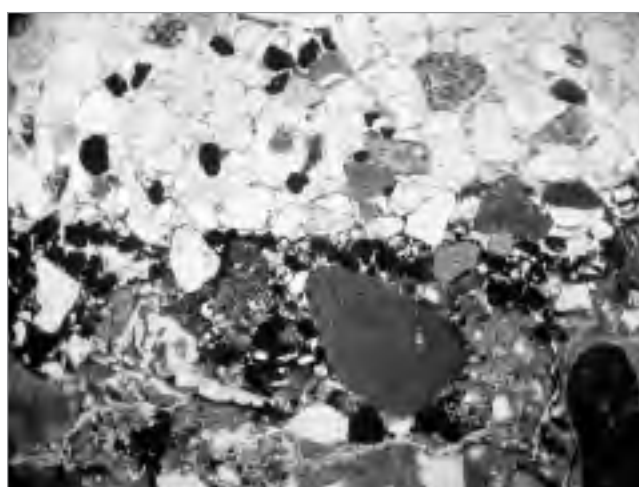


Fig. 21. Gombore I γ , microscopic view of sample 2149, the transition between the archaeological layer and the overlying sands, natural light. *Cliché J.-P. Raynal*

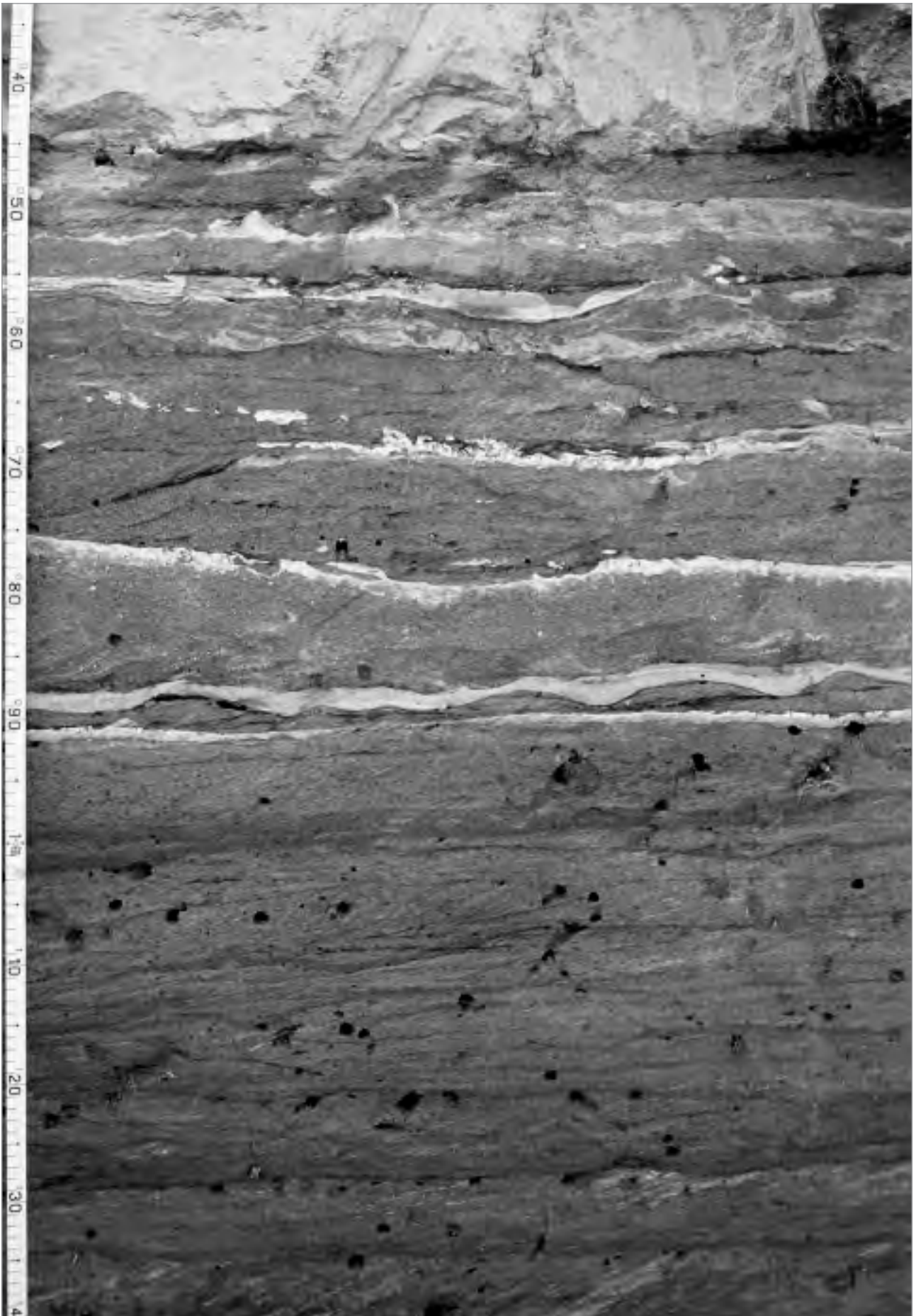


Fig. 22. Gombore Iy. Planar cross-bedded sands above archaeological layer, interbedded with fine redeposited tuffs.

Cliché J.-P. Raynal

The following units have been observed from the bottom to the top of a 2.00 m high section oriented N 45 E and located at the north-west extremity of the main 2002-2003 excavation, between 2020 and 2022 m a.s.l. (Fig. 23). This section is sub parallel to the main axis of a wide channel which dips towards SE and shows clear bank and bed lateral accretion forms (Fig. 31).

- Coarse sands and gravels unit of St to Sp facies (Miall 1996), 0.50 m thick, pumiceous, with tuff soft pebbles; the top bed (sample 2127) is made of well sorted sands ($Md_{\Phi} = 0.40$ and $\sigma_{\Phi} = 0.87$) with a steep unimodal grain-size curve (Fig. 24).
- Unit of Fl facies (Miall 1996), 0.55 m thick, massive silts poorly sorted in the bottom part (sample 2123; $Md_{\Phi} = 5.90$ and $\sigma_{\Phi} = 1.22$) with unimodal grain-size curve (Fig. 24); the upper part is made of poorly sorted silts too (sample 2122; $Md_{\Phi} = 5.95$ and $\sigma_{\Phi} = 1.77$), with small ripples underlined by fine sand micro-beds or by coarser poorly sorted sand lenses (sample 2121; $Md_{\Phi} = 2.40$ and $\sigma_{\Phi} = 1.82$) with a bimodal grain-size curve (Fig. 24).

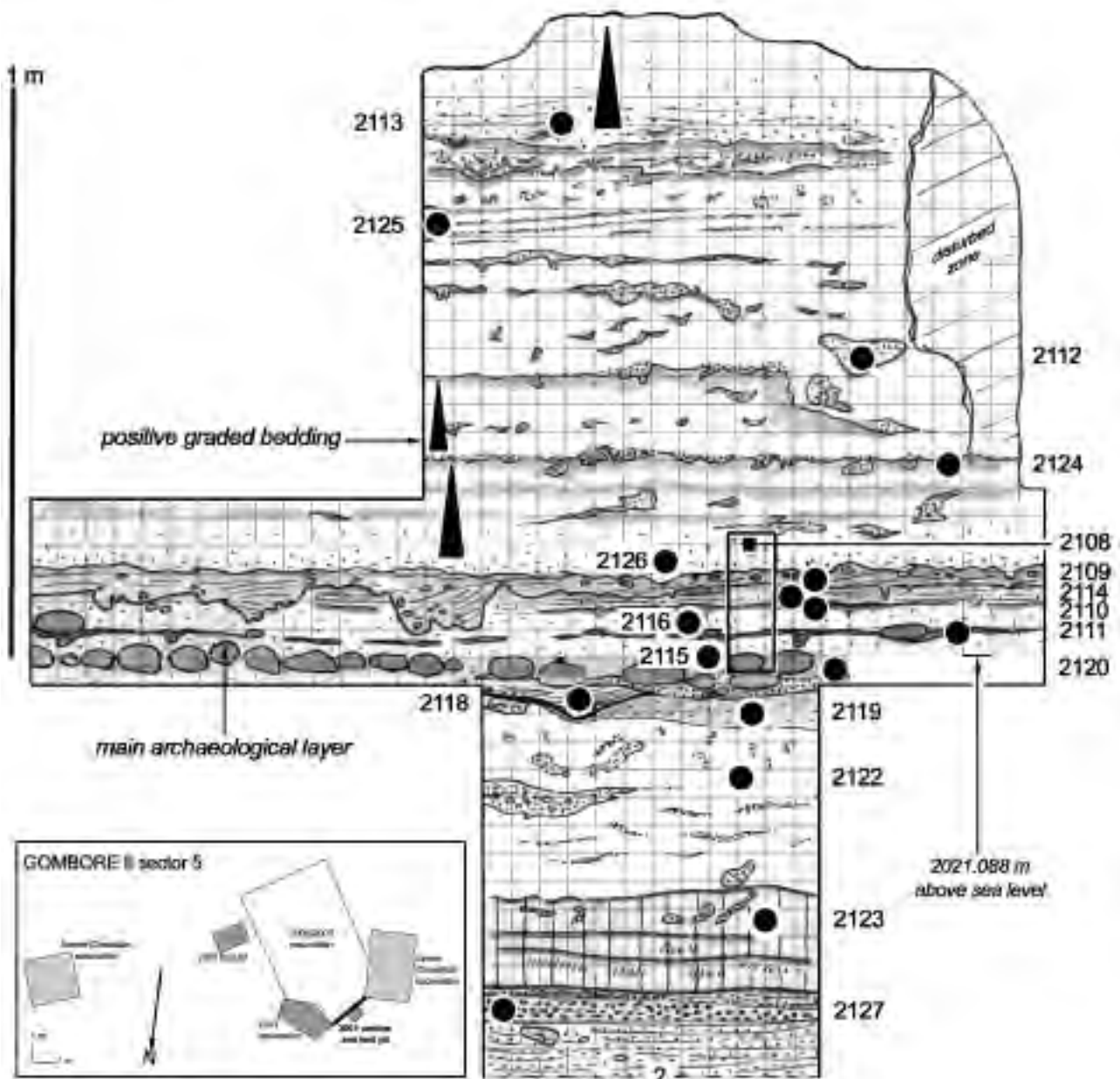


Fig. 23. Gombore II, sector 5. Section with sampling locations: black dots are sediment samples in bulk; black rectangle is oriented blocks sample for examination under the microscope.

- Cros-bedded sands, 0.10 m thick, facies St (Miall 1996), well to poorly sorted (samples 2118 and 2120; $Md_{\Phi} = 2.10/1.95$ and $\sigma_{\Phi} = 0.77/1.37$), grain-size curves are unimodal (Fig. 24).
- Clast-supported thin pebble bed, 0.10 m thick, appearing in section as a stone line, Gh facies (Miall 1996) reduced to the smallest expression. Presence of numerous artefacts and bones which form the main archaeological layer at Gombore II sector 5; when the surface of this unit is exposed, elements are imbricated and show sieving features (for example, smallest elements as obsidian handaxes are vertical in voids among the bigger elements). The sandy matrix (sample 2120) is well sorted ($Md_{\Phi} = 2.10$ and $\sigma_{\Phi} = 0.67$) with a unimodal grain-size curve (Fig. 24), identical to the sands below the pebble lag. Towards mid-channel we observe elements from the archaeological layer floating in bedded sands (Fig. 30), demonstrating the polygenic history of the archaeological surface; large and flat artefacts (handaxes and cleavers) and long bones are significantly oriented indicating a NE/E main current direction.
- Sandy complex, 0.15 m thick, horizontally-bedded, Sh facies (Miall 1996), an alternation of very well sorted epiclastites (samples 2111 and 2109; $Md_{\Phi} = 2.80/2.35$ and $\sigma_{\Phi} = 0.47/0.45$) with steep unimodal grain size curves (Fig. 24), and very poorly silty sands to poorly sorted sandy silts (samples 2116 and 2114; $Md_{\Phi} = 4.00/4.90$ and $\sigma_{\Phi} = 2.05/1.95$) with bimodal grain-size curves (Figs. 24 and 32). Under the microscope, minerals (quartz and feldspars) and abundant ore grains (magnetite) characterize the epiclastic laminae (Figs. 26 and 26??). The top bed of this unit erodes deeply the lower beds with narrow V and U shaped micro-channels filled-up with cross-bedded sands.
- Unit of Fl facies (Miall 1996), 1.00 m thick. Poorly sorted sandy-silts (samples 2126 and 2124; $Md_{\Phi} = 4.75/5.45$ and $\sigma_{\Phi} = 1.90/1.70$) with bimodal grain-size curves (Fig. 32) are intercalated with very thin epiclastic sandy layers and form the bottom part of this unit. Upwards poorly sorted silts show discrete small ripples and low-angle cross-beds underlined by fine very well to moderately sorted epi-

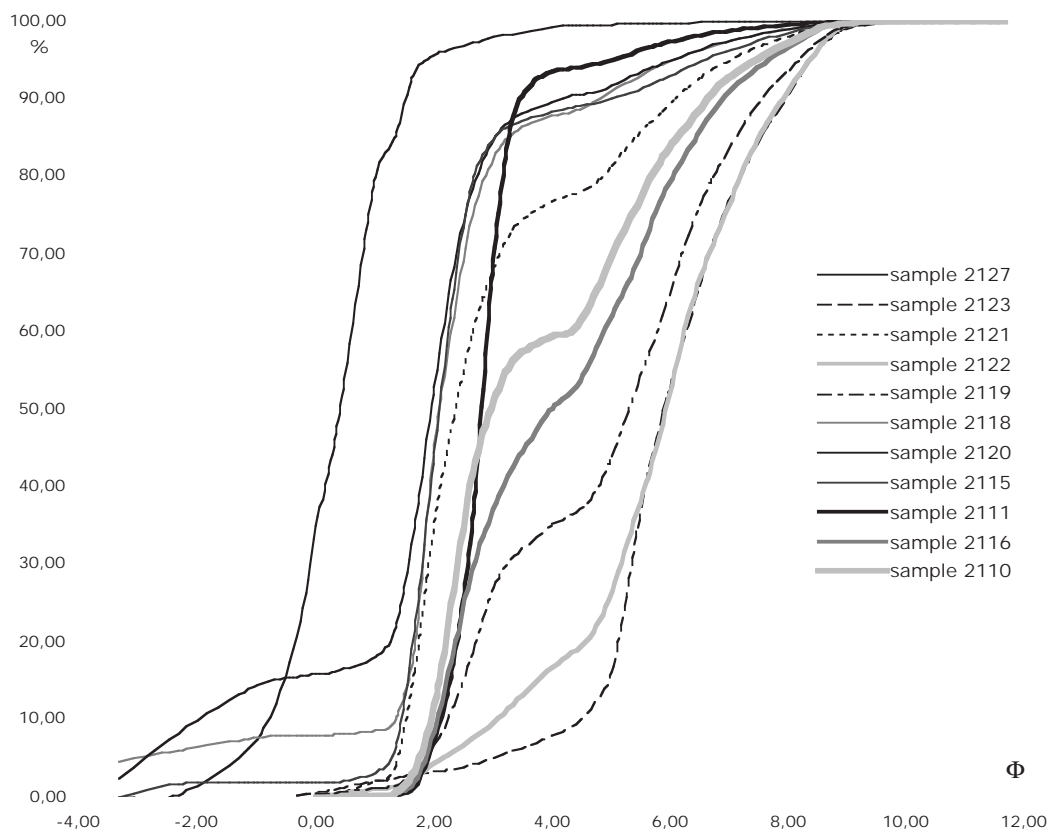


Fig. 24. Gombore II, sector 5. Grain-size curves of the most representative layers up to the archaeological layer and immediately above.

clastic sands (samples 2112, 2113; $Md_{\Phi} = 2.60/ 2.55$ and $\sigma_{\Phi} = 0.42/ 0.85$) with unimodal grain-size curves (Fig. 32). Towards the mid-channel, the epiclastic sandy beds get thicker and we observe a succession of sands and silts identical to the ones described in the preceding sandy complex; under the microscope, sandy beds are a mixture of quartz and feldspars grains with a few ferro-magnesian, some oxidised scoria fragments, pumice and lava fragments; silty beds have matrix-supported finer grains (Figs. 27-29) and are reworked as soft-pebbles (Fig. 31).

Gombore II sector I

The Gombore I excavation located 30 m south of Gombore II sector 5 (Fig. 1) and the section above up to “Butchery site” have been re-examined (Fig. 14). From the bottom to the top, the following succession has been observed.

- Alluvium, cross-bedded coarse pumiceous sands and obsidian gravels, unknown thickness, St to Sp facies (Miall 1996), identical to those described at the base of Gombore II sector 5 section.
- Tuff unit, nearly 1.00 m thick, with vegetal imprints which indicate a fall (re)deposition in water. It is a well sorted silty sand ($Md_{\Phi} = 4.90$ and $\sigma_{\Phi} = 1.83$), geochemistry indicates a dacitic magma (see Raynal and Kieffer in this volume) and it could be “tuff C” of former studies (Chavaillon 1979c; Westphal *et al.* 1979; Cressier 1980).
- Thin bed a few cm thick of coarse moderately sorted sands (sample 9963; $Md_{\Phi} = 1.00$ and $\sigma_{\Phi} = 1.05$; Fig. 33), Sh facies (Miall 1996).
- Clast-supported pebble bed, 0.20 m thick, Gh facies (Miall 1996). Presence of numerous artefacts and bones which form the main archaeological layer (sample 168 in Taieb 1974). The sandy matrix (sample 9958) is well sorted ($Md_{\Phi} = 1.95$ and $\sigma_{\Phi} = 0.65$) with a unimodal grain-size curve (Fig. 33).

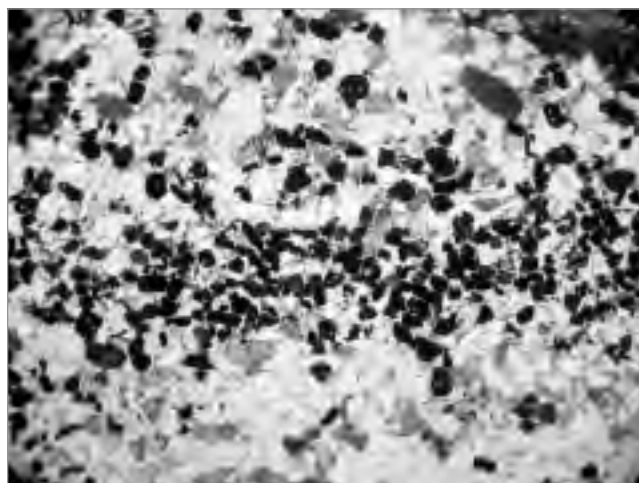


Fig. 25. Gombore II, sector 5, microscopic view of sample 2108 bottom, microbed of opaque minerals.

Cliché J.-P. Raynal

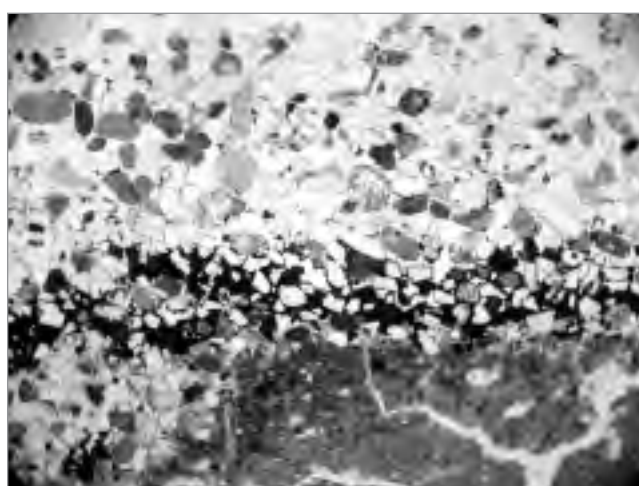


Fig. 26. Gombore II, sector 5, microscopic view of sample 2108 top, reworked tephritic sands with concentration of opaques at the bottom, above silts with dessication cracks.

Cliché J.-P. Raynal

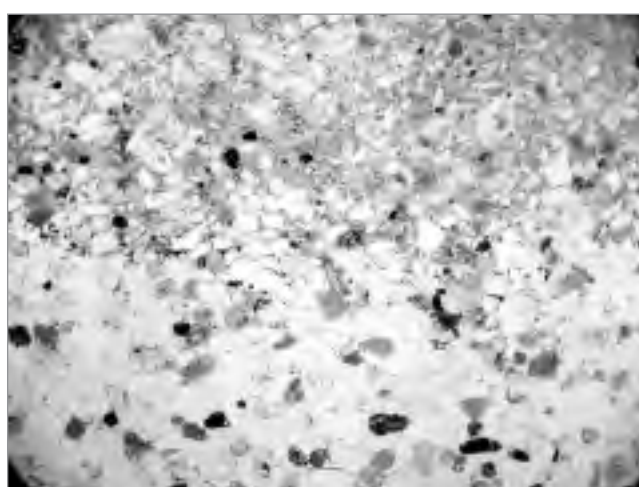


Fig. 27. Gombore II, sector 5, microscopic view of sample 2103 bottom, silts over sands, natural light.

Cliché J.-P. Raynal

- Trachytic tuff unit with vegetal imprints, 0.20 m thick, locally present above the archaeological layer. It is a well sorted sandy silt (sample 9962; Fig. 33; $Md_{\Phi} = 2.60$ and $\sigma_{\Phi} = 1.31$), certainly a fall trapped in water (see Raynal and Kieffer in this volume).
- Silty unit, 2.35 m thick (an equivalent of samples 169/171 in Taieb 1974). The main part shows low-angle cross-bedded to planar bedded SI to Sp facies (Miall 1996), very poorly sorted pumiceous sandy silts (sample 9960; $Md_{\Phi} = 5.55$ and $\sigma_{\Phi} = 2.43$) with a unimodal grain-size curve (Fig. 33). The top part is of Fsm facies (Miall 1996), made of finer still very poorly sorted less sandy silts (sample 9961; $Md_{\Phi} = 6.15$ and $\sigma_{\Phi} = 2.23$; Fig. 33).
- Silty unit, 2.30 m thick, Fm facies (Miall 1996; sample 172 in Taieb 1974), poorly sorted sandy silts with dessication cracks (sample 9956; $Md_{\Phi} = 5.80$ and $\sigma_{\Phi} = 1.88$; Fig. 33).
- Sandy unit, 0.55 m thick, SI facies (Miall 1996), low-angle cross-bedded showing an alternation of very poorly sorted silty sands (sample 9955; $Md_{\Phi} = 3.05$ and $\sigma_{\Phi} = 2.40$) with a bimodal grain-size curve (Fig. 33),



Fig. 28. Gombore II, sector 5, microscopic view of sample 2103 top, sands over silts, natural light.

Cliché J.-P. Raynal

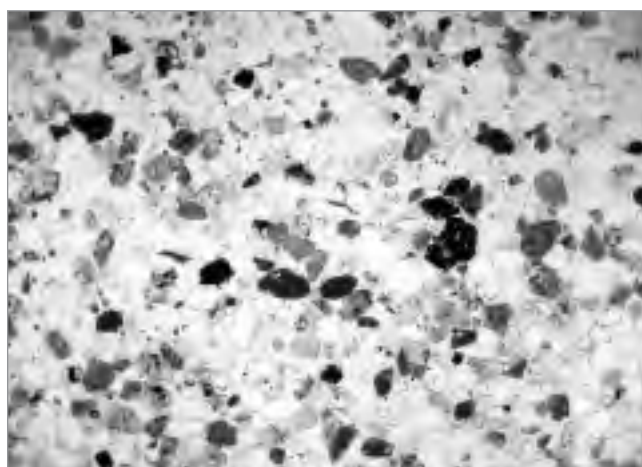


Fig. 29. Gombore II, sector 5, microscopic view of sample 2102 bottom, homometric sands, natural light.

Cliché J.-P. Raynal



Fig. 30. Gombore II, sector 5. Bone floating in laminated sands above the main archaeological layer.

Cliché J.-P. Raynal



Fig. 31. Gombore II, sector 5. Section on north bank of a paleochannel: lateral accretion of sands interbedded with reworked tuffs overlying the main archaeological layer. *Cliché J.-P. Raynal*

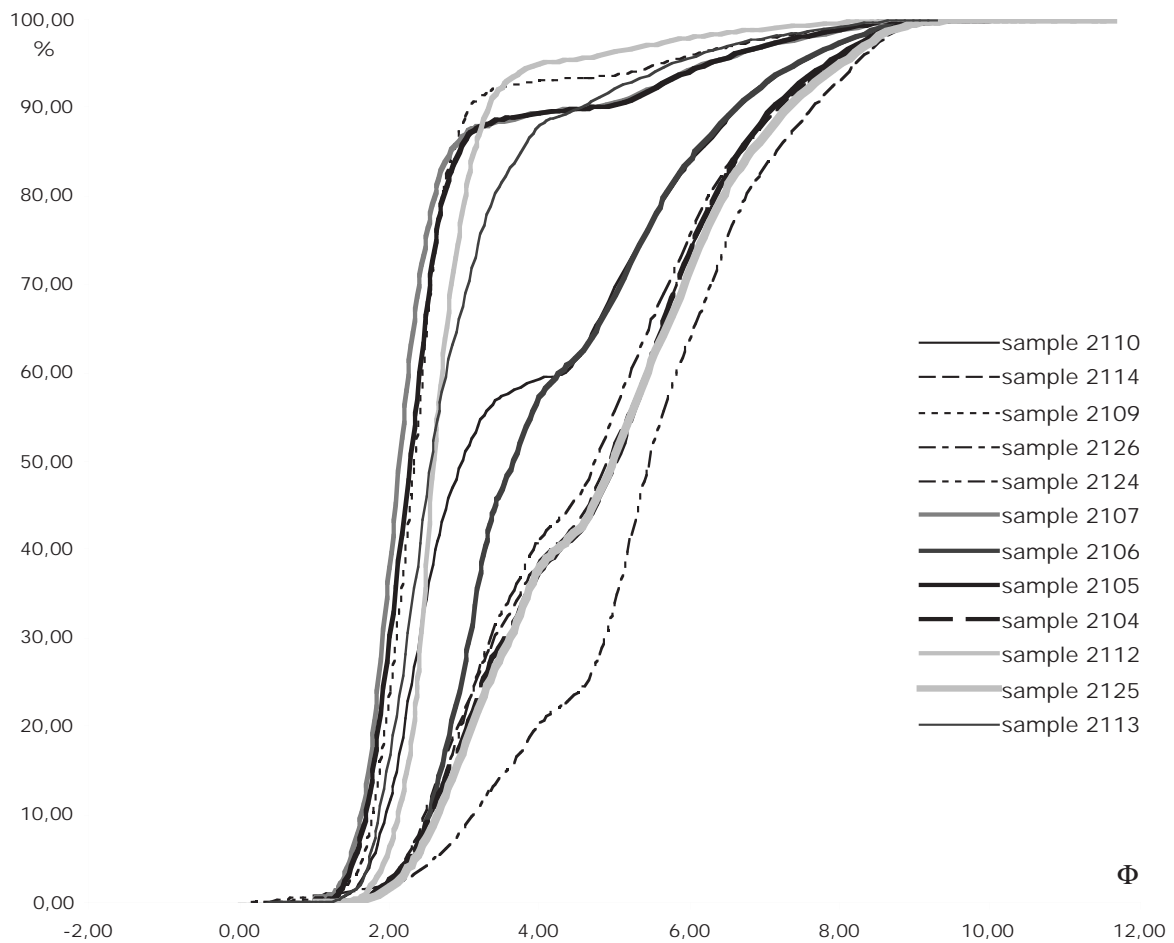


Fig. 32. Gombore II, sector 5. Grain-size curves of the most representative layers above the archaeological layer.

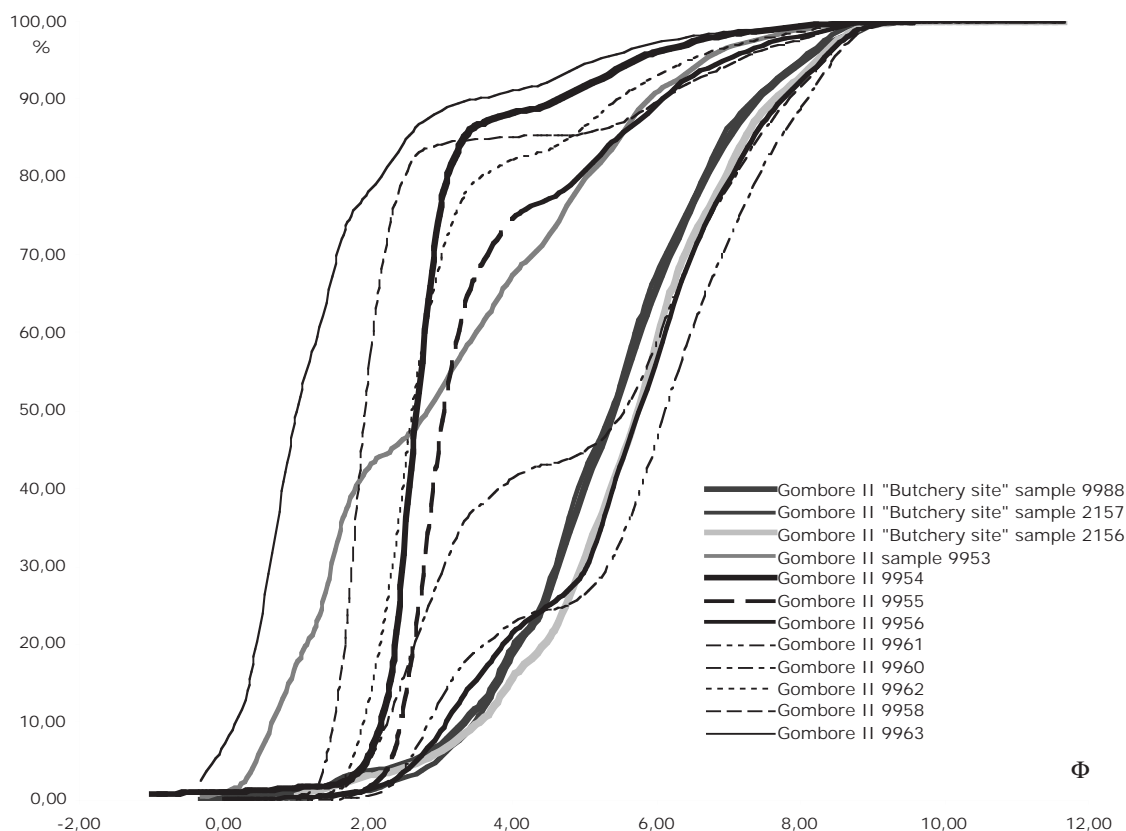


Fig. 33. Gombore II, sector 1. Grain-size curves of the most representative layers above the archaeological layer.

and very well sorted sands (sample 9954; $Md_{\Phi} = 2.65$ and $\sigma_{\Phi} = 0.48$) with a unimodal grain-size curve (Fig. 33).

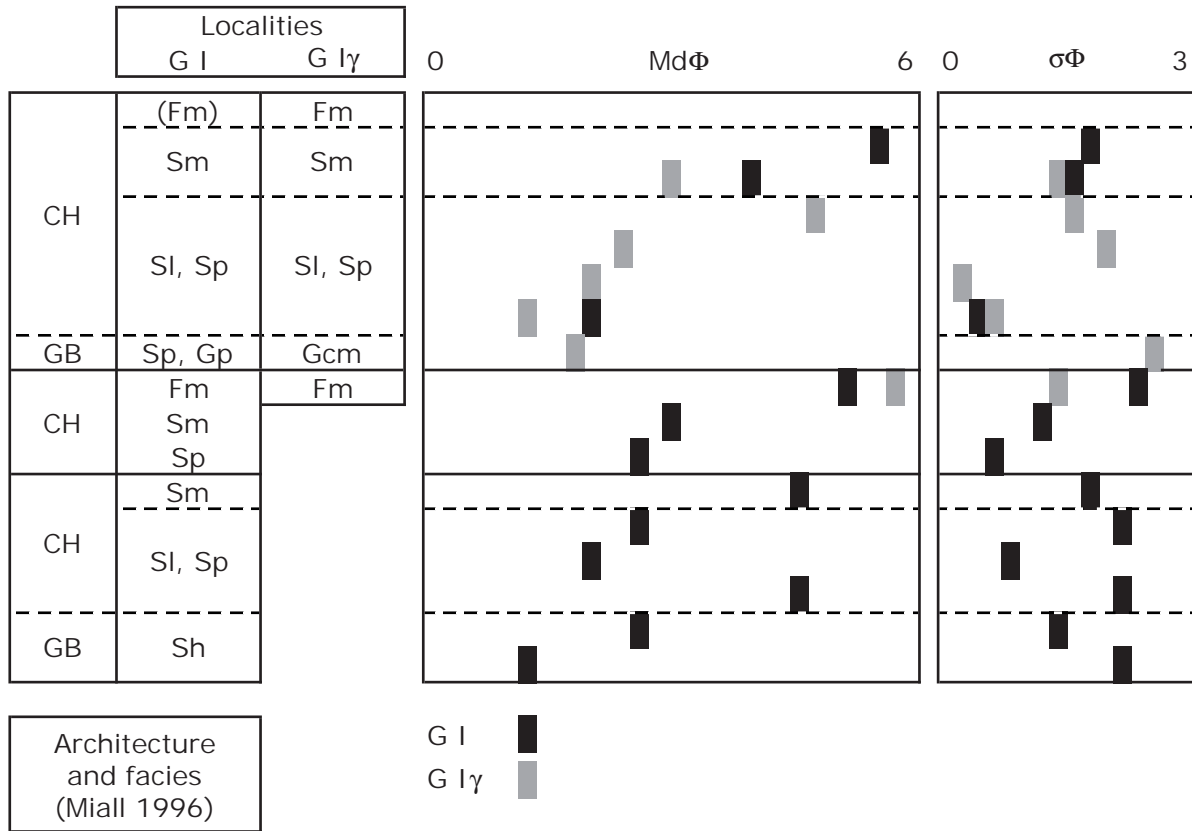
- Sandy unit, 1.00 m thick, Sh to Sl facies, St at top (Miall 1996; possibly sample 176 in Taieb 1974), horizontal to low-angle cross-beds, then trough cross-bed, pumiceous poorly sorted silty sands (sample 9953; $Md_{\Phi} = 2.85$ and $\sigma_{\Phi} = 1.75$) with plurimodal grain-size curve (Fig. 33), bones and lithic artefacts at the bottom of several beds ("Butchery site" lower units).
- Dacitic cinereous tuff, Fsm facies (Miall 1996; possibly sample 177 in Taieb 1974), probably a primary deposit trapped in water, then several episodes of reworking, bone and artefacts at the bottom of the two oldest units ("Butchery site" upper units), silt granulometry, a bit sandy, poorly sorted (samples 2156, 2157, 9988; $Md_{\Phi} 5.40$ to 5.75 and $\sigma_{\Phi} = 1.52$ to 1.57 ; Fig. 33).
- Tuff unit 9989/90: dacitic vesicular tuff and pumice fall (see Raynal and Kieffer in this volume). Probably the same origin than the preceding cinereous tuff.

Preliminary lithostratigraphic synthesis

The lithostratigraphic analysis of the different sections at Garba and Gombore clarify the dynamics nature of the deposition processes for the lower part of the *Melka Kunture Formation*.

Downstream transport and accumulation are prevalent during sedimentation processes. Channel lag petrographic suites reflect the basin geology and indicate a period of global dismantling of ancient volcanic relief and important lateral contributions from both banks' tributaries to alluvial processes (see Bardin *et al.* in this volume). Volcanic activity is the main provider for fine grains sediments: pumice derived from pyroclastites of penecontemporaneous plinian eruptions contribute massively to channel lags and to major

accretion events (Sl, Sp, St facies), reworked coarse tuffs form massive beds (Sm facies) while cinereous tephras are responsible for silts deposition (Fsm, Fm facies). Resistant and opaque minerals form the matrix of bed lags and most of the sandy bases of current structures. Grain-size distribution also reflects the evolution of channels (Tab. 2).



Tab. 2. Grain-size characteristics of the lower part of *Melka Kunture Formation* at Gombore I.

At Gombore (Tab. 3), six channels are superposed and partly embedded. Each of them exhibits a logical facies succession leading to complete infilling and abandonment while the main stream migrates towards SE. Archaeological layers are systematically associated with the bedforms, except for the uppermost one. The volcanic input is responsible for overloading of streams and forces channel changes. Facies previously considered as lacustrine (Taieb 1974) are actually fluvial facies. The “major cut-and-fill” previously considered as major erosion phases by Chavaillon (1973) are only simple channeling processes.

At Garba IV (Tab. 4), three channels are superposed and partly embedded. Each of them exhibits a logical facies succession leading to a complete infilling and eventual abandonment. Archaeological layers are associated with the bedforms, local erosional surface or temporary abandoned channel. The volcanic input is systematically responsible for over-loading and forces channeling. Here again, facies previously considered as lacustrine are actually fluvial and the “major cut-and-fill” previously considered as important erosional phases are only simple channeling processes.

Considering the paleomagnetic data and especially the brief normal polarity event (Jaramillo Polarity Subzone, 1.07 to 0.99 Ma) recognized both at Garba in the upper part of “Tuff A” and at Gombore Iγ at the top of sands above the archaeological layer (Cressier 1980), the preliminary absolute dating (Schmitt *et. al.* 1977) and the revisited tuff correlations (see Raynal and Kieffer in this volume), it can be concluded that both series deposited between 1.77 Ma (end of Oldoway Polarity Subzone) and 0.78 Ma (Brunhes-Matuyama limit) at most.

Architectural elements (after Miall 1996)	Facies at Gombore I (after Miall 1996)	volcanic input archaeology	Facies at Gombore Iy (after Miall 1996)	volcanic input archaeology	Facies at Gombore II sector 5 (after Miall 1996)	volcanic input archaeology	Facies at Gombore II sector 1 (after Miall 1996)	volcanic input archaeology
CH							tuff 9989/90	V
LA / CH							Fsm Sh, Sl, St	A
GB							Sl	A
CH	?						Fm	
GB	(tuff 9978/86)	V					Fsm	
CH	?						Sl, Sp	
GB			Sm				tuff 9962	V
CH	(Fm)	V	Gcm				Gh	A
GB	Sm	V	Fm				Sh	
CH	Sl, Sp	V	Gcm	V				
GB	Sp, Gp	V	Fm	V				
CH	Fm		Gcm					
CH	Sm		Fm					
CH	Sl, Sp							
GB	Sh, G							
GB	tuff 9945/47	V						
	Sh, G	O						

LA	lateral accretion
CH	channels
GB	gravel bars and bedforms
v	redeposited tuff
V	direct tuff
A	Acheulian layer
O	Oldowan layer

Tab. 3. Architecture and facies of the *Melka Kunture Formation* at Gombore I and II.

Architectural elements (after Miall 1996)	Facies at Garba IV (after Miall 1996)	volcanic input archaeology	former tuff names
CH	Sm tuff 9931/34 Sl, Sp	V	"C tuff)
CH	Sm ? St	A	
CH	Sm, Fsm tuff 9928/29 ?	V	"B tuff"
LA / CH	Sr, Sl St	v	"A tuff"
CH	tuff 9919/18 Sh, Sr St, Sr, Sh, Sm	V	"A0 tuff"
GB	Gcm/Gh	v	
		v	
CH	Sm tuff 9911 Sm, Sh, Sl	V	"Grazia tuff"
		v	
		O	

Tab. 4. Architecture and facies of the *Melka Kunture Formation* at Garba IV.

Architectural elements (after Miall 1996)	Facies at Gombore I (after Miall 1996)	volcanic input archaeology	Facies at Gombore Iy (after Miall 1996)	volcanic input archaeology	Architectural elements (after Miall 1996)	Facies at Garba IV (after Miall 1996)	volcanic input archaeology	former tuff names
CH	(Fm) Sm	v	Fm	v	CH	Sm, Fsm tuff 9928/29	V	"B tuff"
GB	Sl, Sp Sp, Gp	V	Sm Sl, Sp Gcm	V	LA / CH	?	A	"A tuff"
CH	Fm Sm Sp		Fm	A	CH	St tuff 9919/18	V	"A0 tuff"
CH	Sm Sl, Sp Sh, G				CH	Sh, Sr St, Sr, Sh, Sm	v	
GB	tuff 9945/47 Sh, G	V	Gombore IB	O	GB	Gcm/Gh Sm	O	Garba IV D
		O			CH	tuff 9911 Sm, Sh, Sl	V	"Grazia tuff"
							v	O

Tab. 5. Attempt at correlation between Garba IV and Gombore I series.

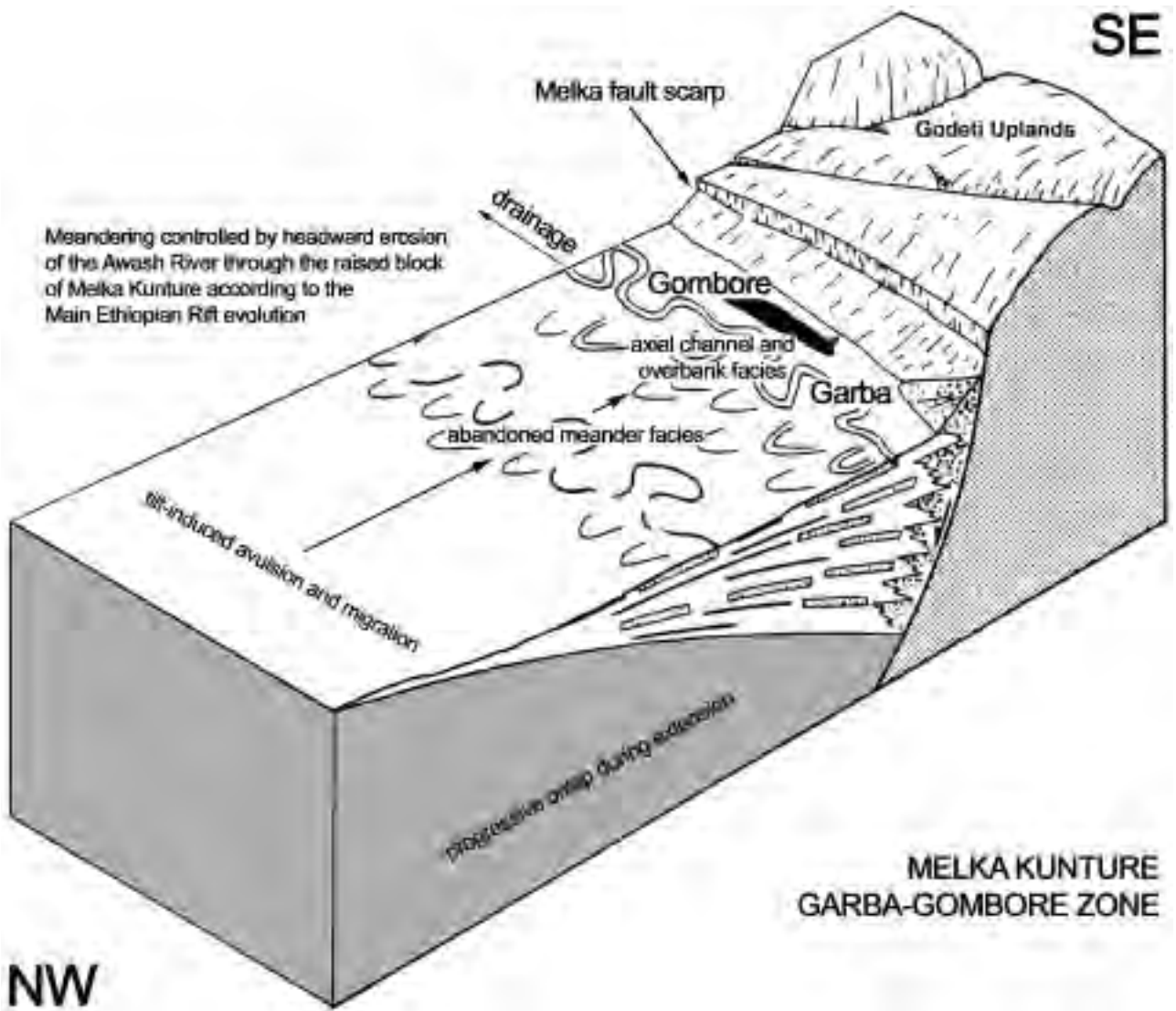


Fig. 34. The *Melka Kulture Formation* at Garba-Gombore: a shallow seasonal braided river environment in a half-graben basin with axial through drainage during Lower and Lower-Middle Pleistocene (modified after Miall 1996, and Leeder and Gawthorpe 1987).

In such fluvial deposits, preservation of archaeological or tuff units is localized and chancy. Thus correlations between distant sections are difficult to establish. An attempt at correlation is nevertheless proposed for the basal units of both localities (Tab. 5) which is not far from that established by Taieb (1974).

From an archaeological perspective, Oldowan and Acheulian sites are associated with bedforms and gravel bars. These layers have been affected by currents (sieve effect, re-orientation of large pieces) and repeatedly washed and covered by abrasive sands during accretion or subjected to erosional episodes which have highly disturbed the primary organisation of artefacts. This is clearly attested by taphonomic studies (see Fiore and Tagliacozzo in this volume).

The superposition of the different facies clearly indicates a tectonic control of the sedimentation for the *Melka Kunture Formation* (at least for its lower terms described in this paper) during the Lower Pleistocene: the recurrent faulting (moderate subsidence of the semi-graben) along the Melka scarp which borders the Garba-Gombore area is directly responsible for this architecture.

A pause in subsidence combined with head erosion through the Melka Kunture raised block allowed a return to valley incision processes and installation of valley-plain and stopped terraces fossilized by the non-welded ignimbrite episode (see Raynal and Kieffer in this volume), significantly wide-spread and thus named *Kella Formation* (Fig. 2). This unit belongs clearly to the Matuyama Polarity Zone with a minimum age of 0.78 Ma. The setting of this ignimbrite seems to have fit into a topography close to the present one. After the emplacement of the non-welded ignimbrites a fault reactivation takes place with an important displacement (see Raynal and Kieffer in this volume).

The meandering of the palaeo-Awash was certainly determined by the obstacle of the raised block of Melka Kunture according to the Main Ethiopian Rift evolution (see Bardin *et al.* in this volume). Combined head erosion and subsident faulting are responsible for the successive changes in sedimentation style such as channeling, superposition or down-cutting when volcanic input increases deposition rates and forces channeling changes. The different facies identified indicate a shallow, seasonal, low-sinuosity, braided river environment (Fig. 34). This is indicative of a well-contrasted dry-wet seasonal climate. Further investigations will certainly render these preliminary conclusions more precise.

Acknowledgements

Financial support for field work and laboratory analyses was provided by GDR CNRS *Hommes et volcans avant l'histoire*, Région Aquitaine and Région Auvergne for project *Espaces volcaniques préhistoriques* and Italian Archaeological Mission at Melka Kunture. We are grateful to Marianne Hirbec-Raynal for the English translation and to Peter Bindon for its revision. We thank Mosshine El Graoui who prepared the thin sections.